Intra- and Inter-Rater Reliability in the Cross-Sectional Area of Feline Epaxial Musculature on CT Scan

Thesis

Presented in Partial Fulfillment of the Requirements for the Degree Master of Science in the Graduate School of The Ohio State University

By

Laura Rayhel, DVM

Graduate Program in Comparative and Veterinary Medicine

The Ohio State University

2020

Thesis Committee

Jessica Quimby

Valerie Parker

Rachel Cianciolo

Julie Byron

Eric Green

Abstract

INTRODUCTION AND BACKGROUND:

The initial chapters of this thesis will introduce the importance of evaluating cachexia and muscle loss in patients with chronic disease, definitions of terminology associated with muscle mass loss and disease, cellular pathways and mechanisms by which chronic kidney disease leads to loss of muscle, and current modalities by which skeletal muscle amounts can be quantified.

OBJECTIVES:

The aim of this study was to evaluate the intra- and inter-rater reliability of epaxial muscle cross-sectional area measurement on feline CT images and to determine the relationship between normalized epaxial muscle area (EMA) and subjective muscle condition score (MCS).

METHODS:

Feline transverse CT images including the junction of the 13th thoracic vertebrae/13th rib head were retrospectively reviewed. Right and left epaxial muscle circumference and vertebral body height were measured and an average normalized EMA (ratio of epaxial area:vertebral height) was calculated for each image. Measurements were performed by three individuals blinded to the clinical data and were repeated 1 month later. Intra- and inter-rater reliability of EMA was assessed with concordance

correlation coefficient (CCC), and Bland-Altman analysis was performed to assess bias and limits of agreement (LoA) between and within observers at different time points. In cats for which MCS data were available, EMA was compared between differing MCSs via the Kruskal-Wallis test, with Bonferroni-corrected Wilcoxon rank-sum post-hoc analysis.

RESULTS:

In total, 101 CT scans met the inclusion criteria for reliability analysis, 29 of which had muscle condition information available for analysis. Intra-rater EMA CCC ranged from 0.84 to 0.99 with minimal bias (range -0.16 to 0.08) and narrow LoA. Inter-rater EMA CCC ranged from 0.87 to 0.94, bias was larger (range -0.46 to 0.66) and LoA were wider when assessed between observers. Median EMA was significantly lower in cats with severe muscle atrophy (2.76, range 1.28-3.96) than in all other MCS groups (P <0.0001 for all comparisons).

CONCLUSIONS AND RELEVANCE:

Measurement of EMA on CT showed strong intra-rater reliability, and median EMA measurements were significantly lower in cats with severe muscle wasting, as assessed on physical examination. Further studies correlating EMA to lean muscle mass in cats are needed to determine whether this method may be useful to quantify muscle mass in patients undergoing a CT scan. Further studies are needed to identify the best clinical modality to quantify skeletal muscle in veterinary patients, and to evaluate possible interventions which could stop or slow progression of cachexia.

Acknowledgments

The author would like to acknowledge the members of her Thesis Committee, Drs. Jessica Quimby, Julie Byron, Valerie Parker, Rachel Cianciolo, and Eric Green, for their support and guidance through this project. She would also like to acknowledge her family members, Matt King, Elizabeth Rayhel, and Harry Rayhel, without whom this project would not have been possible.

Special thanks to Leeah Whittier and Linda Costanzo for their permission to use the illustrations in this text.

Vita

Small Animal Rotating Internship, Purdue University – West Lafayette, Indiana
Doctor of Veterinary Medicine, University of Missouri – Columbia, Missouri
Bachelor of Science, Fontbonne University, St. Louis, Missouri
Bachelor of Science, Washington University, St. Louis, Missouri

Publications

1. Rayhel LH, Quimby JM, Green EM, Parker VJ, Bai S. Intra- and inter-rater reliability in the cross-sectional area of feline lumbar epaxial musculature evaluated via abdominal CT scan. J Feline Med Surg. 2019:1098612X19880997.
2. Rayhel L, Aitken-Palmer C, Joyner P, Cray C, Lizarraga CA, Ackerman B, et al. Hematology and Biochemistry in Captive White-Naped Cranes (Grus Vipio). J Zoo Wildl Med. 2015;46(4):747-54.
3. Shane DT, Rayhel LH, Huang Z, Zhao J-C, Tang X, Stavila V, et al. Comprehensive NMR Study of Magnesium Borohydride. The Journal of Physical Chemistry C. 2011;115:3172-7.
4. Rayhel LH, Corey RL, Shane DT, Cowgill DF, Conradi MS. Hydrogen NMR of Palladium Hydride: Measuring the Hydride−Gas Exchange Rate. The Journal of Physical Chemistry C. 2011;115:4966-70.
5. Shane DT, Corey RL, Rayhel LH, Wellons M, Teprovich Jr. JA, Zidan R, et al. NMR Study of LiBH4 with C60. The Journal of Physical Chemistry C. 2010;114:19862-6.
6. Shane DT, Corey RL, McIntosh C, Rayhel LH, Bowman Jr. RC, Vajo JJ, et al. LiBH4 in Carbon Aerogel Nanoscaffolds: An NMR Study of Atomic Motions. The Journal of Physical Chemistry C. 2010;114:4008-14.

Fields of Study

Major Field: Comparative and Veterinary Medicine

Table of Contents

List of Tables

List of Figures

Chapter 1. Introduction

"Cachexia" generally refers to a loss of muscle mass and has been described in multiple disease processes in humans and companion animals.[1] It may seem obvious that people, cats, and dogs with chronic diseases lose weight, muscle mass, and strength. Indeed, the first description of cachexia in the medical literature comes from Hippocrates in Ancient Greece: "The flesh is consumed and becomes water, ⋯ the abdomen fills with water, the feet and legs swell, the shoulders, clavicles, chest and thighs melt away ⋯ This illness is fatal."[1] However, the detrimental effects of loss of muscle on patient outcome, even before reaching the level of severity described by Hippocrates, on patient outcome are only now being elucidated.

Numerous studies in humans have established cachexia, decreased strength, and/or unintended weight loss as an independent risk factor for death, adverse events, and disease progression in chronic kidney disease, chronic obstructive pulmonary disease, and multiple cancers.[2-11] Aside from its effects on mortality and outcome, decreased muscle mass and strength are associated with loss of quality of life in older adults.[12] In dogs, loss of skeletal muscle has been associated with decreased survival in congestive heart failure.[13] In a study in cats with a diagnosis of neoplasia, muscle wasting was present, and decreased body condition and body weight were found to be negative

prognostic indicators for remission and survival.[14] However, muscle condition was not included in the survival analysis. Another study evaluating the effect of body weight and body condition on survival of cats with heart failure identified a 'U-shaped' correlation between body weight and survival, in which cats with the lowest and highest body weights had the highest risk of death, but muscle condition was not evaluated in those cats.[15] Analysis of body weight's effect on survival in cats with chronic kidney disease showed a similar 'U-shaped' relationship; cats with the highest and lowest body weights at diagnosis had the highest risk of death.[16] Again, muscle condition was not evaluated in this study. A very recent study evaluated survival time in cats with congestive heart failure, according to seven different definitions of cachexia extrapolated from humans. When muscle condition was used as the defining factor, 46% of cats with congestive heart failure were cachectic, and the median survival time in cachectic cats was shorter by almost 100 days.[17]

Further studies investigating cachexia in companion animals with chronic diseases are indicated, as studying and identifying mechanisms associated with cachexia may identify interventions to prevent it or slow its progression. However, performing such research requires a repeatable, objective measure of skeletal muscle quantity. Early or subtle decreases in skeletal muscle may be difficult to detect via changes in body weight alone. Decreases in skeletal muscle may also occur simultaneously with increases in fat mass, leading to stable or minimally affected body weight despite progressive losses of muscle. Body weight is also affected by pathologies such as dehydration, effusion or tumor growth, which may confound identification of losses in fat and muscle mass. Body

condition scoring systems are designed to detect losses in fat mass and may miss decreases in skeletal muscle mass, especially if subtle.[18] Muscle mass, specifically, can be evaluated on physical examination using the muscle condition scoring (MCS) system described by Michel et al.[18] However, this system is subjective and showed only modest correlation to lean body mass as determined by dual x-ray absorptiometry (DEXA, described in later chapters).[18] The World Small Animal Veterinary Association (WSAVA) has also published guidelines for qualitative muscle condition scoring based on Michel's system; however, the same concerns for subjectivity and poor correlation to reference standards (such as they are) remain for this system.[19] In humans, imaging modalities such as muscle group ultrasound, abdominal MRI, and abdominal CT have been used to create estimates of whole-body skeletal muscle mass.[20-36] In veterinary medicine, these modalities are not yet well-established to evaluate skeletal muscle. Clearly, more objective and accessible assessments of muscle condition are needed before reliable research into the mechanisms behind and effect of cachexia on morbidity and mortality in chronic disease can progress.

This thesis will review definitions associated with cachexia and muscle loss in aging and disease states, known mechanisms by which chronic disease may predispose patients to developing cachexia, as well as methods used in human medicine to quantify skeletal muscle mass and volume for cachexia detection. It will also describe one of the first forays into the use of CT scan for evaluation of skeletal muscle quantity in cats. The aim of this thesis is to give the reader a background in definitions associated with cachexia/sarcopenia, mechanisms by which cachexia occurs in chronic kidney disease,

and to establish whether CT evaluation of feline epaxial muscles can be performed repeatably within/between observers. A secondary aim is to establish the relationship between CT-evaluated feline epaxial muscle cross-sectional area and muscle condition assessed on physical examination.

Chapter 2. Definitions and Terminology

Terminology used to describe weight loss associated with age and chronic disease has varied widely, hampering the ability to compare scientific findings across studies and disciplines. When this phenomenon was initially identified, no clear vocabulary existed for clinical features of weight loss, fat loss, and/or muscle mass loss associated with age, decreased nutrient intake, or chronic disease states. Terms such as malnutrition, cachexia, weight loss, wasting, and others were used without definitive characteristics for each. Recently, however, consensus groups have sought to unify the language used to describe these clinical phenomena. The following chapter reviews the current definitions for common terms used to describe age- and disease-associated tissue wasting in human medicine, and discusses potential applications to veterinary medicine, where no consensus definitions currently exist. Notably, general definitions for these terms have been defined, while clinical definitions that can be used to definitively determine the presence or absence of these types of tissue wasting still vary somewhat among consensus groups. In veterinary medicine, no clinical consensus definitions for malnutrition, sarcopenia, cachexia, or protein-energy wasting currently exist.

Malnutrition

A recent consensus statement from the European Society of Clinical Nutrition and Metabolism (ESPEN) attempted to clarify and define terminology related to nutrition and weight/muscle loss.[37] In this document, "malnutrition" is defined as a "state resulting from lack of intake or uptake of nutrition that leads to altered body composition (decreased fat free mass) and body cell mass leading to diminished physical and mental function and impaired outcome from disease".[37] In simpler terms, malnutrition can refer to a lack of intake of nutrients, such as in starvation or anorexia, *or* metabolic derangements that result in altered nutritional needs that are not met by the individual patient's diet. Malnutrition can be associated with starvation, advanced aging, or disease, or a combination of these factors.[37] The resulting alterations in body composition can lead to the outcomes of secondary sarcopenia, protein-energy wasting, and cachexia (defined below), and are associated with an increased risk of adverse outcomes and mortality, regardless of the underlying reason that the patient became malnourished in the first place.[37]

An earlier consensus statement from the same group outlined diagnostic criteria that established a clinical definition of malnutrition. Two alternative definitions of malnutrition were proposed:[38]

- Definition 1: Body mass index (BMI) [weight in kg/(height in m)^2] < 18.5 kg/m^2

or

- Definition 2: Unintentional weight loss > 10%, or > 5% in 3 months, in combination with either
    - BMI < 20 kg/m^2 (< 70 years of age); BMI < 22 kg/m^2 (≥ 70 years of age)

      or
    - FFM index (FFMI) [FFM in kg/(height in m)^2] < 15 kg/m^2 (women) or 17 kg/m^2 (men)

Fat-free mass (FFM) in this definition was measured by validated technical devices such as bioelectrical impedance (BIA) or dual-energy x-ray absorptiometry (DEXA), or imaging techniques such as computed tomography (CT), ultrasound (US), or magnetic resonance imaging (MRI).[38] Techniques to measure FFM are discussed in later chapters.

Note that under definition 2, unintentional weight loss and loss of FFM (i.e. skeletal muscle) are sufficient to define malnutrition, regardless of loss or gain of fat mass. Also note that both definitions identify cut points for normal BMI and FFMI, which are problematic in veterinary patients as breed-, sex-, neutering status-, and age-specific reference intervals for BMI and FFMI are not established. As such, this paper will adhere to the general definition of malnutrition described in the first paragraph.

Simple & Stressed Starvation

"Simple starvation" refers to the body's normal response to short-term or prolonged fasting in the absence of underlying disease.[39] In the short-term (< 72 hours), insulin secretion diminishes as glucagon and catecholamine secretion increase, leading to

glycogenolysis, lipolysis, triglyceride hydrolysis and release of free fatty acids and glucose which are used for energy. In the longer term, glycogen stores are depleted, and hepatic and renal gluconeogenesis maintain blood glucose. Glucose is synthesized from amino acids, glycerol from adipose tissue, and lactate from muscle anaerobic metabolism. To decrease consumption of amino acids and protein, metabolic rate decreases 10-15% (via reduction of thyroid hormone and catecholamine secretion) and the body and brain adapt to using a higher proportion of ketones from free fatty acid beta oxidation for energy. These adaptations can decrease protein catabolism by up to two-thirds.[39]

In "stressed starvation", ongoing inflammation or critical illness prevent the adaptive responses to fasting described above, leading to ongoing protein catabolism in preference to adipose tissue and ketone use for energy.[39] The underlying disease causing maladaptive protein catabolism commonly induces anorexia or hyporexia as well, leading to a vicious cycle of malnutrition and ongoing loss of muscle.[37, 40-42] With time, stressed starvation will lead to the clinical outcomes of sarcopenia and cachexia, described below.

Sarcopenia

Generally, sarcopenia refers to loss of muscle mass, strength, and function.[37, 43-48] Initially, consensus definitions differed as to whether the term "sarcopenia" was reserved for age-related loss of FFM in the absence of disease, or referred to FFM loss secondary to any cause. he newest definitions in human medicine now differentiate muscle loss secondary to age (primary sarcopenia) and secondary to disease and other factors like

disuse or malnutrition (secondary sarcopenia) within this term.[37, 45, 47] Notably, sarcopenia by itself is not associated with weight loss, as increased fat mass, tumor burden, or fluid retention can offset the loss of muscle mass and result in stable weight.[49] If such an offset is occurring, identification of early sarcopenia can be clinically challenging.

Unfortunately, clinical definitions of sarcopenia vary according to measures used to determine muscle mass and function as well as cut-points to define presence/absence and stages of sarcopenia. More recent definitions in human medicine have focused on loss of muscle strength and decline in physical function, rather than loss of overall muscle mass, as the principal determinant of sarcopenia.[46] Most clinical definitions use a combination of estimated muscle mass and tests of muscle strength, physical function, or both.[45, 46, 50] For example, the consensus statement from the European Working Group on Sarcopenia in Older People (EWGSOP) defines sarcopenia according to the following factors:[45, 46]

- DEXA-assessed skeletal muscle mass index (appendicular skeletal muscle mass/height) < 7.0 - 7.26 kg/m^2 (men) or < 5.5 kg/m^2 (women)
- Grip strength < 27 - 30 kg (men) or < 16 - 20 kg (women)
- Short physical performance battery score (SPPB) ≤ 8
    - Composite score including balance, gait speed, and time to rise from sitting to standing 8 times
    - Some studies use gait speed < 0.8 m/s alone[45]

The EWGSOP consensus statement also includes gradations for sarcopenia based on bioimpedance analysis, and distinguishes “pre-sarcopenia” from “sarcopenia” and

"severe sarcopenia" based on whether the patient has loss of muscle mass, strength, physical performance, or all three.[45] Regardless of definition, sarcopenia was associated with decreased quality of life, injury, and all-cause mortality in older adults.[12, 51] The ESPEN consensus statement also cites the above parameters to define sarcopenia clinically.[37]

Computed tomography is also commonly used to assess skeletal muscle quantity (discussed further in later chapters). For example, a recent study in healthy Korean adults proposed age-specific cutoff values for sarcopenia using estimated cross-sectional area of the psoas muscle at the level of the third lumbar vertebra, adjusted for patient height (termed the psoas muscle index, or PMI) as follows.[26]

Table 1: Proposed Age-Specific Cutoff Values for Psoas Muscle Index in Korean Adults.

Age Group (years)	Male Cutoff Value (mm^2/m^2)	Female Cutoff Value (mm^2/m^2)
< 40	592.3	399.9
40-49	474.0	287.7
50-59	422.2	242.5
60-70	374.4	220.4
> 70	331.5	147.6

Clearly, similar age- and sex- specific cutoff values are needed for other ethnic groups before such cut-points can be used widely in the general patient population. Note that cut-off values decrease with each age group in both sexes, and that the difference between male and female cutoff values also decreases with age.[26] Another study in obese cancer patients used skeletal muscle cross-sectional area at L3 on CT scan, normalized by body

surface area, to predict total body skeletal muscle and determined cutoffs for sarcopenia based on survival analyses.[22] This study proposed 52.4 cm^2/m^2 in men, and 38.5 cm^2/m^2 in women, to define sarcopenia in this patient population.[22]

Validation of specific definitions of sarcopenia is complicated by the lack of a "gold-standard" definition for sarcopenia and the use of different outcome parameters in different studies. A comparison of agreement between various definitions for sarcopenia revealed only slight-moderate agreement between most definitions.[50] As such, there is no working "gold-standard" clinical definition of sarcopenia in human medicine. Certainly, there is no clinical definition that lends itself to extrapolation to veterinary medicine, as all use measures such as gait speed, grip strength, BMI, or FFMI that do not translate or are not currently established for veterinary patients. Within the research that has been performed in veterinary medicine, definitions of "sarcopenia" mainly adhere to the definition of primary sarcopenia listed above. Namely, "sarcopenia" in veterinary medicine traditionally refers to muscle mass associated with aging in the absence of disease.[52] Therefore, we will adhere to this definition for the purposes of this paper.

Sarcopenic Obesity

It is important to note that obesity and sarcopenia are not mutually exclusive. "Sarcopenic obesity" refers to a state in which aging or underlying disease leads to progressive loss of lean body mass while excessive fat mass is preserved or increased.[45, 53, 54] Sarcopenia can be more difficult to identify in obese individuals, but obesity itself may contribute to

sarcopenia development by increasing fat infiltration into muscle, release of adipose-associated inflammatory mediators, insulin resistance, promoting a sedentary lifestyle, and further lowering physical function.[46, 53] Unfortunately, no consensus clinical definition currently exists for sarcopenic obesity in human medicine.

Protein-Energy Wasting

In the literature, "protein-energy wasting" (PEW) refers to "the state of decreased body stores of protein and energy fuels (that is, body protein and fat masses). This abnormality is often associated with diminished functional capacity related to metabolic stresses."[55] Thus, PEW represents a change in energy stores (protein and adipose tissue) that can lead to sarcopenia/cachexia in late stages, and specifically deals with an absolute or relative decrease in protein intake compared to the body's needs.[56, 57] PEW occurs secondary to states of disease or chronic inflammation, and can result in loss of both fat and muscle.[55, 58, 59] In PEW secondary to disease, the condition cannot be reversed by providing increased nutritional supplementation, unless the underlying disease that led to PEW is also addressed.[60]

Most of the literature on PEW deals specifically with chronic kidney disease (CKD), although scoring systems used in a recent meta-analysis to establish PEW have also been applied to patients with other diseases.[59] Such scoring systems include the seven-point "subjective global assessment of nutritional status" (SGA)[61] and the "comprehensive malnutrition-inflammation score" (MIS).[62] Both the SGA and MIS apply subjective

scores for unintentional weight loss, qualitative decreases in dietary intake, gastrointestinal symptoms, qualitative decreases in physical function, and decreases in fat and muscle mass assessed on physical examination.[61, 62] The SGA additionally assigns points for severity of edema and a subjective rating for "overall nutritional status".[61] The MIS also accounts for years on dialysis and severity of comorbidities, as well as quantitative measures of body mass index (BMI) [weight in kg/(height in m)^2], serum albumin, and serum total iron binding capacity.[62] In general, to meet criteria for PEW, unintentional weight loss, muscle mass loss, and low dietary protein intake occur, with possible subsequent decreases in albumin.[57] In general, PEW criteria include loss of muscle and body weight, even if absolute cut-off points for low muscle mass or BMI have not yet been reached.[57] Thus, it could be said that PEW occurs prior to, and eventually results in, losses of muscle mass and function severe enough to be termed "cachexia".

The above scoring systems could be extrapolated to veterinary patients but have yet to be validated in dogs and cats. In this paper, PEW will refer to a combination of metabolic and appetite derangements that predispose the patient to losses of lean body mass with or without fat mass losses. The pathophysiology of PEW will be discussed extensively in later chapters.

Cachexia

Cachexia refers to a "complex metabolic syndrome associated with underlying illness and characterized by loss of muscle with or without loss of fat mass."[45] Like PEW, cachexia is not reversible by improved nutritional intake, without first correcting the underlying disease process causing the cachexia.[49, 63] Cachexia may be considered a subset of secondary sarcopenia, in which loss of muscle mass and strength is associated with underlying chronic disease and inflammation and excludes "normal" muscle loss associated with starvation or aging. Indeed, the recent ESPEN consensus statement on nutrition terminology in human medicine advocates for the use of "cachexia" interchangeably with "chronic disease-related malnutrition (DRM) with inflammation."[37] DRM with inflammation/cachexia is considered distinct from "non-DRM" such as hunger or starvation, and from "DRM without inflammation" which encompasses diseases that cause mechanical decreases in nutrient intake (i.e. dysphagia, neurologic disorders, or dementia).[37] Note that non-DRM and DRM without inflammation would result in decreased absolute intake of nutrients, but, at least in early stages, would not be expected to result in malabsorption, maldigestion, or metabolic derangements that affect nutritional needs, appetite, or muscle/energy homeostasis (discussed in later chapters). As such, the exaggerated loss of muscle mass and function in excess of loss of fat stores for energy occurs only in cachexia, and does not occur in states of decreased nutritional intake in the absence of underlying disease, at least not until very late stages.[45]

Like sarcopenia, many clinical definitions for cachexia have been proposed, and no "gold standard" clinical definition currently exists in the human literature.[37, 41, 42, 47, 49, 63-65] The ESPEN consensus statement suggests applying the same absolute criteria as for malnutrition (see above), with the caveat that a simultaneous disease or biochemical indices indicative of inflammation [increased C-reactive protein (CRP); decreased albumin] must also be present.[37] Other studies make use of similar parameters used to define sarcopenia above, in the presence of chronic disease.[63] Scoring systems have been devised that use weight or weight loss, body composition and muscle function tests like grip strength, hematologic and biochemical parameters such as hematocrit, lymphocyte count, albumin, interleukin (IL)-6, CRP, prealbumin, lactate, and others, as well as patient questionnaires to establish the diagnosis.[40, 41, 64] Still other studies include no measure of skeletal muscle mass or function in their definition, using only weight loss and BMI to determine whether cachexia is present.[42] Again, regardless of the definition used, none lends itself readily to extrapolation to cats and dogs. As such, "cachexia" in this paper will refer to disease-associated loss of muscle mass, strength, or function, regardless of fat mass.

Cachexia is considered the end-stage of PEW in some studies,[55-57] although other studies attempt to define a less severe state, "pre-cachexia", which may be considered similar to PEW. In pre-cachexia, unintentional weight loss and appetite derangements are already occurring, and an underlying chronic disease or systemic inflammation must be present.[47] Note the similarities in this definition to the parameters of the SGA and MIS scoring systems used for PEW in the above section. Some studies, mainly centered in cancer-

associated cachexia, also define a more severe category, termed “refractory cachexia”, characterized by severe weight loss and low BMI.[42, 63]

For clarification of the interrelationships of each of the above terms, refer to Figure 1. These relationships will define the use of each of these terms for the remainder of this paper.

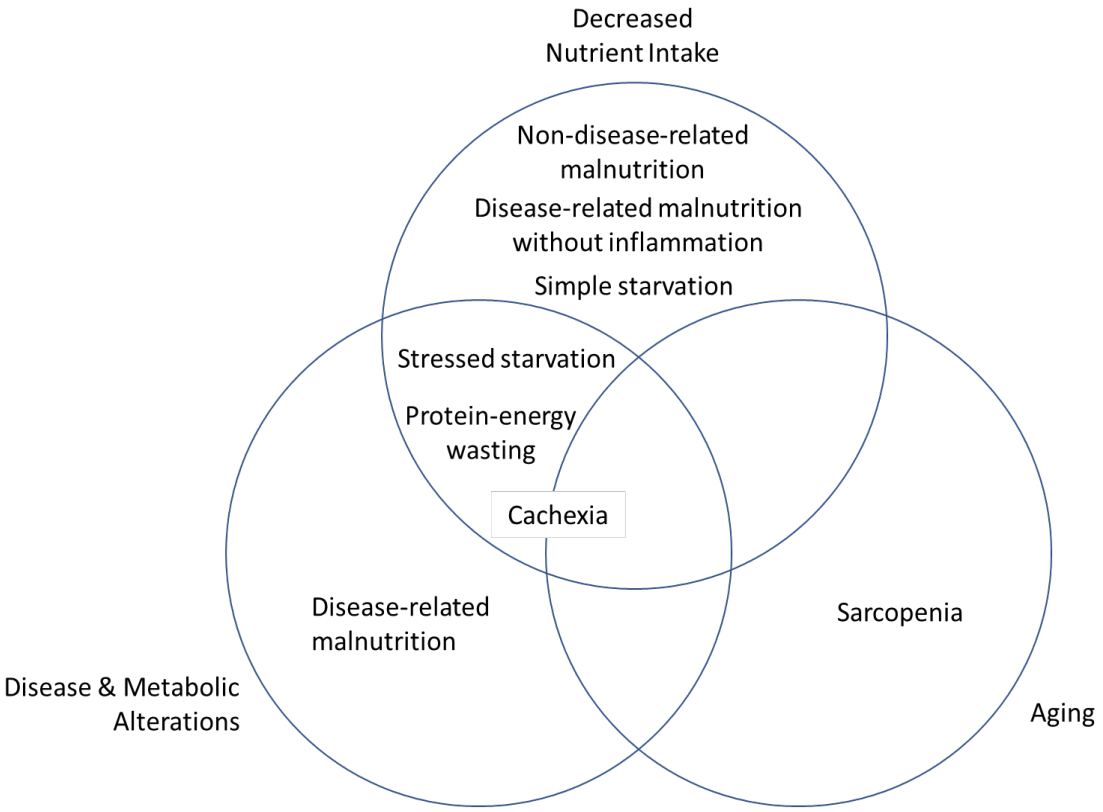

Figure 1: Interrelationships between terminology used to describe weight and muscle loss in states of altered nutritional & disease status.

Chapter 3. Skeletal Muscle Physiology, Hypertrophy, and Atrophy

Skeletal muscle functions to create movement and force, maintain posture, determine basal energy metabolism, and produce heat to maintain core body temperature.[66] It contains 50-75% of all body proteins, accounts for 30-50% of whole-body protein turnover, and acts as an important reservoir for amino acids used by other organs and tissues.[66] At all times, protein synthesis and degradation are occurring within muscle fibers; the strength and quality of skeletal muscle is the result of a balance between these two opposing processes.[67] This balance is affected by a number of external and internal factors, including exercise and physical activity, diet, neuronal input, muscle fiber type, mitochondrial number and location, and hormonal inputs.[67] The following chapter will review the normal structure and physiology of skeletal muscle, and explore the cellular pathways that promote muscle synthesis and degradation.

Review of Skeletal Muscle Structure & Physiology

Individual skeletal muscles are comprised of groups of muscle "fascicles", each of which is composed of multiple muscle cells, called "muscle fibers" or "myocytes."[68] The skeletal muscle as a whole is surrounded by a connective tissue sheath called the "epimysium"; connective tissue around each fascicle is termed the "perimysium", and

connective tissue around each muscle fiber is termed "endomysium."[68] In turn, each muscle fiber contains multiple nuclei (myonuclei), mitochondria, and many long, filamentous protein structures arranged in parallel called "myofibrils", each of which runs nearly the length of the muscle itself (Fig. 2).[68, 69]

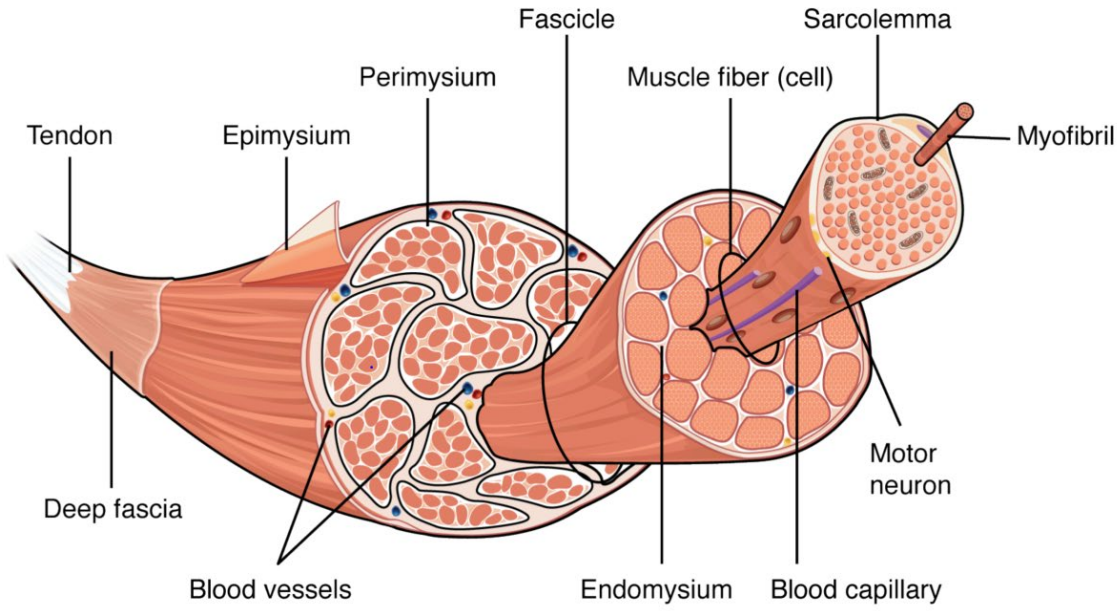

Figure 2: Structure of skeletal muscle. (From: Biga et al.[69] [Fig. 10.21])

The myofibrils consist of individual subunits, called "sarcomeres", which are arranged in series and are responsible for muscle contraction in response to an action potential. The sarcomeres are composed of protein "filaments"; a "thick filament" composed of "myosin", and a "thin filament" which is a complex of the proteins "actin", "tropomyosin", and "troponin". Troponin is composed of three subunits, I, C, and T. These proteins are arranged to form the thick and thin filaments as shown in Figure 3.[70]

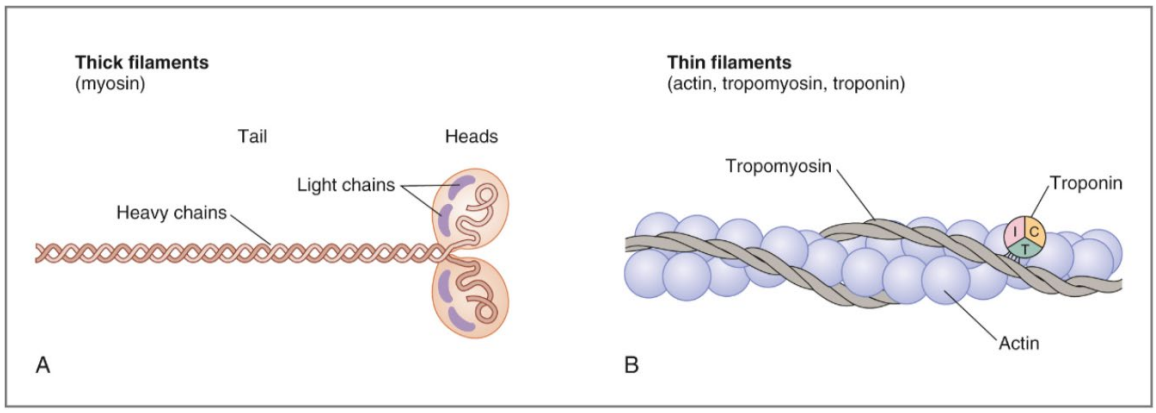

Figure 3: (A) Structure of the thick filament of skeletal muscle. (B) Structure of the thin filament of skeletal muscle. (From: Costanzo, L[70] [Fig. 1.21])

Note that in the above figure, the myosin molecule ends in two "heads", and that the tropomyosin molecule is wound about the chain of actin molecules, binding the troponin complex and holding it in place. "Active sites" on the actin molecule chain are hidden underneath the troponin complex; these active sites can bind with the myosin heads if the troponin complex is moved out of the way.[70, 71] The thick and thin filaments are arranged within the sarcomere as shown in Figure 4,[70] and the myofibrils are composed of multiple sarcomeres in sequence.

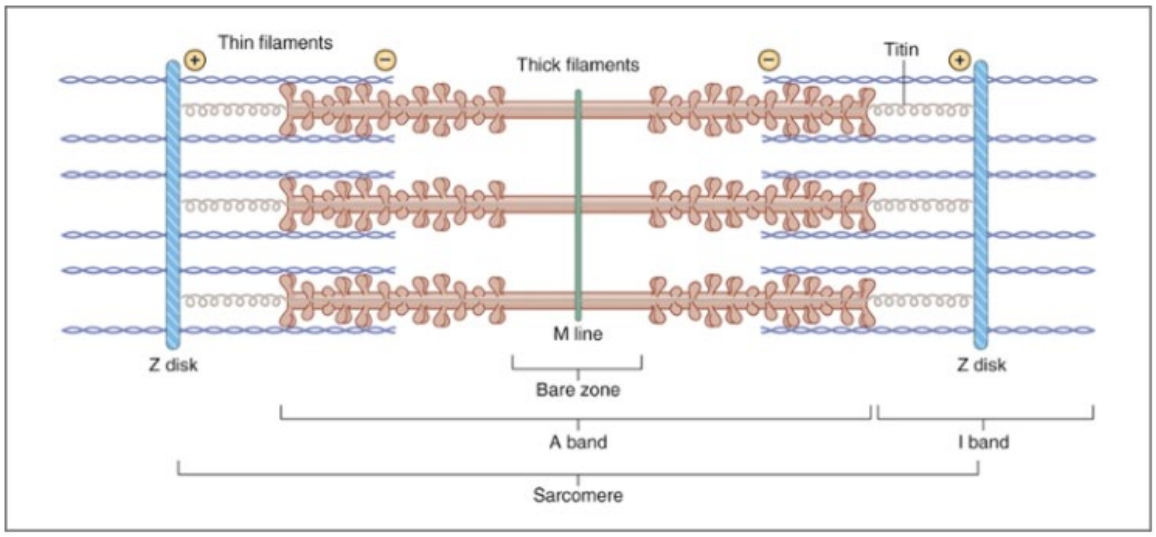

Figure 4: Structure of a sarcomere. (From: Costanzo, L[70] [Fig. 1.22])

Within the myocyte, specialized, calcium-containing "sarcoplasmic reticulum" (SR) winds in tubules that surround the individual myofibrils, ensuring that calcium release from the SR in response to an action potential rapidly exposes the sarcomeres to large numbers of calcium ions, which bind the troponin C subunit. This causes a conformational change in the tropomyosin molecule which "uncovers" the active sites on the actin molecule, allowing them to bind with the nearby myosin heads in the sarcomere.[70, 71] In the presence of adenosine triphosphate (ATP), this begins a process called "cross-bridge cycling", which allows for contraction of the myofibril.

Cross-bridge cycling will continue as long as calcium is bound to the troponin C subunit of the light chain complex and ATP is still available. The actin and myosin molecules will be dragged across each other, overlapping more and more until cross-bridge cycling

ceases. When combined across multiple myofibrils, this process will result in shortening of the whole muscle and contraction.[66, 70, 71]

Relaxation of the myofibril will not occur until intracellular calcium levels fall to baseline ($< 10^{-7}$ M). Calcium decreases as the Ca^{2+} ATPase of the sarcoplasmic reticulum (SERCA) pump returns calcium to the interior of the SR. When intracellular calcium levels are insufficient to bind troponin C, tropomyosin resumes its previous conformation, once again blocking the active sites of the actin filament from access to the myosin heads.[70]

Skeletal muscle has been classified according to multiple different criteria throughout its study, including color, myoglobin content, fatiguability, calcium handling by the SR, and others.[66] Currently, three classification schemes exist: classification based on staining for the ATPase molecule on the myosin head, classification based on the isoform of myosin molecule present in the myofibril, and classification based on predominant energy metabolism used (glycolysis vs. oxidative phosphorylation).[72] Generally three basic muscle fiber types exist, based on multiple characteristics:[66, 71]

Table 2: Classification of Muscle Fiber Types.

Fiber Type	Contraction Speed	Predominant Pathway for ATP Synthesis	Myoglobin Content	Fatiguability	Mitochondria
I	Slow	Oxidative	High	Low	Many
IIa	Fast	Mixed*	Low	Intermediate	Few
IIx/IIb	Fast	Glycolytic*	Low	High	Few
*Variability in metabolism exists for IIa and IIx/IIb fiber types					

The specific molecular characteristics of the myosin filaments in each type confer these differences in contraction speed.[66] While a good correlation exists between type I myosin heavy chain isoform-containing fibers and oxidative metabolism, not all IIa fibers have mixed oxidative-glycolytic metabolism, and not all IIx/IIb fibers have glycolytic metabolism.[72] Importantly, different fiber types respond differently to processes such as exercise, nutrient depletion, denervation, and aging.[67]

Muscle growth occurs mainly through hypertrophy of individual myocytes, and only rarely through hyperplasia. Generally, hypertrophy involves a greater rate of synthesis actin and myosin filaments; filament number can increase by as much as 50% when hypertrophy is occurring.[71] By contrast, disuse and other factors will lead to muscle fiber atrophy, in which the rate of actin and myosin degradation exceeds the rate of synthesis. Satellite cells, the adult stem cells of skeletal muscle, are present between myocytes and can proliferate and differentiate into new myocytes for muscle growth, repair, and regeneration.[66] In some conditions such as hypertrophy associated with exercise and

muscle damage, satellite cell activation and the addition of new myonuclei may occur; however the contribution of satellite cell recruitment to myofiber hypertrophy is currently controversial.[67, 73, 74] Specific pathways associated with atrophy and hypertrophy are discussed in the next section.

Signaling Pathways Promoting Skeletal Muscle Growth & Hypertrophy

mTOR Pathway

Mammalian target of rapamycin (mTOR), an intracellular serine/threonine kinase, is a major regulator of skeletal muscle mass, especially as it relates to resistance training and recovery from atrophy.[67, 73] mTOR exists in complexes with other protein components. The hypertrophic effects of mTOR complex 1 (mTORC1), a complex of proteins including mTOR and "raptor", a scaffold protein which regulates substrate binding and complex assembly, are best elucidated.[67, 73, 75, 76] However, mTORC2, containing a different scaffold protein called "rictor", may also have pro-synthetic effects are not yet fully understood.[77] For the purposes of this paper, we will focus on mTORC1 signaling.

mTORC1 has myriad downstream effects depending on effector molecule and cell type, including appetite regulation, adipogenesis, lipogenesis, insulin regulation, lysosomal regulation, and oncogenesis.[75] In skeletal muscle, the effector mechanisms of mTORC1's anabolic effects are incompletely characterized.[67, 75] However, the most likely effectors of mTORC1 in affecting protein translation are phosphorylation of a serine/threonine protein kinase called $p70^{S6K1}$, phosphorylation of an inhibitory protein called 4E-BP1,

and potentially, increased synthesis of protein subunit eIF2Bε of the eIF2B holoenzyme.[73]

Activation of $p70^{S6K1}$ increases ribosomal translation of mRNA into proteins via multiple mechanisms, inhibits degradation of certain pro-synthetic proteins by the ubiquitin proteasome system (described below), increases biogenesis of ribosomes, and increases synthesis of pyrimidine DNA and RNA nucleotides.[73] 4E-BP1 inhibits recruitment of the 40S ribosomal subunit for initiation of protein translation, until phosphorylated by mTORC1.[73] Hypophosphorylated 4E-BP1 also inhibits translation of certain mRNAs with specific characteristics of their 5'-untranlsated regions including cyclin D1, c-Myc and ornithine decarboxylase, which play a role in mechanically-induced hypertrophy of skeletal muscle.[73] Thus, phosphorylation of 4E-BPI by mTORC1 increases RNA transcription and protein translation. The eIF2B holoenzyme delivers the initiator tRNA to the 40S ribosomal subunit, a crucial step in initiation of protein translation; availability of the eIF2Bε subunit may be the rate-limiting factor in protein synthesis.[73] Thus, activation of mTORC1 produces multiple downstream effects to upregulate RNA synthesis, increase protein translation rate and capacity, and potentially to upregulate specific synthesis of pro-hypertrophic proteins in skeletal muscle.[73]

In addition to its effects on protein anabolism, mTORC1 also upregulates transcription of mitochondrial genes.[78] Likely, these effects are mediated through mTORC1 activation of peroxisome-proliferator-activated receptor coactivator (PCG)-1α, allowing it to interact with a transcription factor, Yin Yang 1 (YY1).[78] In complex, these proteins upregulate

transcription of multiple genes involved in oxidative phosphorylation, the tricarboxylic acid cycle, and uncoupling mitochondrial respiration for heat production.[78] mTORC1 activation also increases glycolytic energy metabolism via increased synthesis of hypoxia inducible factor 1α.[75] Therefore, as mTORC1 activation drives protein synthesis and energy consumption, it also increases ATP synthesis by both oxidative and glycolytic pathways.

mTOR, potentially in both the mTORC1 and mTORC2 complexes, also has inhibitory effects on protein degradation and autophagy pathways (discussed below) which may also contribute to hypertrophy.[77] For example, mTORC1 phosphorylates and inhibits both unc-51-like kinase 1 (ULK1) and Atg13, two key components to autophagy initiation.[79, 80] However, further studies are needed to evaluate mTOR's role in regulating the protein degradation pathways that we will discuss in later sections.

mTORC1 is activated by multiple stimuli. One prominent activation pathway is the insulin-like growth factor 1/phosphoinositide-3-kinase-Akt/protein kinase B-mammalian target of rapamycin (IGF-1/PI3K-Akt/PKB-mTOR) pathway.[67, 81] IGF-1 is a 7.5 kD protein in the somatomedin family which is synthesized by multiple body tissues in response to stimulus by pituitary growth hormone.[82, 83] IGF-1 secretion, and therefore mTOR activation, decreases during fasting, when insulin concentrations in the portal vein are low, and increases with protein intake.[83-85] IGF-1 receptors are located on the cells of multiple body tissues, and initiate intracellular signaling pathways involved in protein synthesis, cellular hypertrophy and division, and avoidance of apoptosis.[85] PI3K

(activated through stimulation of insulin receptor substrate (IRS)-1 by the IGF receptor) acts as the major intracellular signal promoting protein synthesis in response to IGF-1 binding its receptor in multiple cell types throughout the body.[85] Activation of PI3K then stimulates Akt (also known as protein kinase B), which in turn inhibits a molecule called tuberin, or tuberous sclerosis 2 (TSC2). Inhibition of TSC2 activates Rheb (Ras-homolog expressed in the brain), which in turn activates mammalian target of rapamycin (mTOR).[73] Akt also inhibits pras40, a molecule which inhibits mTORC1 activity through interactions with the raptor protein.[79] Thus, activation of Akt by PI3K relieves mTORC1 inhibition. Muscle hypertrophy in response to β-adrenergic agonists and androgen hormones also occurs via Akt-mediated mTORC1 activation.[67]

Increases in extracellular amino acid concentrations, in particular leucine and arginine, also activate mTORC1 independently of the Akt pathway. This occurs via processes that recruit inactive mTORC1 to the surface of intracellular lysosomes, where activation occurs.[75, 79] mTORC1 activation also occurs with mechanical loading of muscle, such as resistance exercise. This activation also appears to occur via pathways other than the IGF-1 pathway described above, although the extracellular signals by which mTOR "senses" mechanical loading are currently controversial.[73]

Importantly, suppression of mTORC1 signaling occurs under multiple types of cellular stress, including energy/ATP depletion, hypoxia, proteotoxic stress (buildup of misfolded proteins), damage or dysfunction of the endoplasmic reticulum, osmotic disequilibrium, DNA damage, and oxidative stress.[79, 86] This makes physiologic sense, as reduction in

mTORC1 activity would lead to energy conservation and a reduction in the synthesis of misfolded proteins.

Notably, while multiple studies indicate the importance of mTOR signaling for muscle hypertrophy in response to resistance exercise, and for muscle regeneration, mTOR's involvement in basal protein synthesis rates and maintenance of existing muscle mass is less clear.[73]

Signaling Pathways Promoting Skeletal Muscle Atrophy

Atrophy, the shrinkage of myofibers, results from multiple processes, including disuse, starvation/malnutrition, and denervation. Atrophy occurs due to loss of proteins, mainly myofibrillar components including the light and heavy chains of myosin, actin, and structural sarcomeric proteins. Organelles and cytoplasm are also lost in atrophy.[67] Skeletal muscle atrophy occurs via two major mechanisms: the ubiquitin-proteasome system (UPS), and the autophagy-lysosome pathway (ALP).[74] Both systems interact to result in a net loss of protein mass within the myocyte.

Ubiquitin-Proteasome System

Ubiquitin is single-chain polypeptide found in most cell types, and the addition of ubiquitin in specific conformations to an existing intracellular protein marks that protein for proteasomal destruction. The ubiquitination process involves three main steps, requiring sequential actions from three enzymes, categorized into E1, E2, and E3 groups.

E1 enzymes activate ubiquitin, then conjugate it onto the active site of an E2 (conjugating) enzyme. E3 ubiquitin ligases bind the target protein and the E2 enzyme to transfer activated ubiquitin onto the target.[74] The 26S proteasome consists of a cylindrical structure with six, interiorly-facing proteolytic active sites, capped by narrow pores at each end of the cylinder which bind ubiquitin, allowing entry of the protein for degradation.[87] Prior to degradation, de-ubiquitinating enzymes remove the bound ubiquitin molecules, which are then recycled for additional use.[74]

In humans, there are more than 600 E3 ubiquitin ligases, each of which may bind one or multiple substrates.[88] Diversity within the E3 enzyme group allows the UPS system to have multiple specific targets within the cell. Several E3s have been found to be upregulated in conditions associated with muscle atrophy, including disease states, fasting, and disuse in mouse models, and certain genes encoding specific E3s are known to have substrates specific for components of the sarcomere.[74] These include muscle RING finger 1 (MuRF1)/Trim63, atrogin-1/MafBx/Fbxo32, Trim32, and possibly Nedd4-1. MuRF1 ubiquitinates troponin I, as well as several components of the myosin thick filament, including myosin heavy chain, myosin light chains 1 & 2 (see Figure 3), and myosin-binding protein C, which recruits creatine kinase to myosin filaments in the sarcomere.[74] Components of the thin filament, including actin, tropomyosin, and the troponins, are targeted by Trim32, which also ubiquitinates α-actinin and desmin, components of the Z-disk which anchors the myosin filaments within the sarcomere (see Figures 4 and 5). Atrogin-1 also targets structural Z-disk components including desmin and vimentin. Nedd4-1 may, in turn, target the proteins that assemble the actin filament,

leading to depletion, rather than degradation, of sarcomeric proteins.[74] See Figure 5 for a visual representation of these E3 ligases and their targets within the sarcomere.[74]

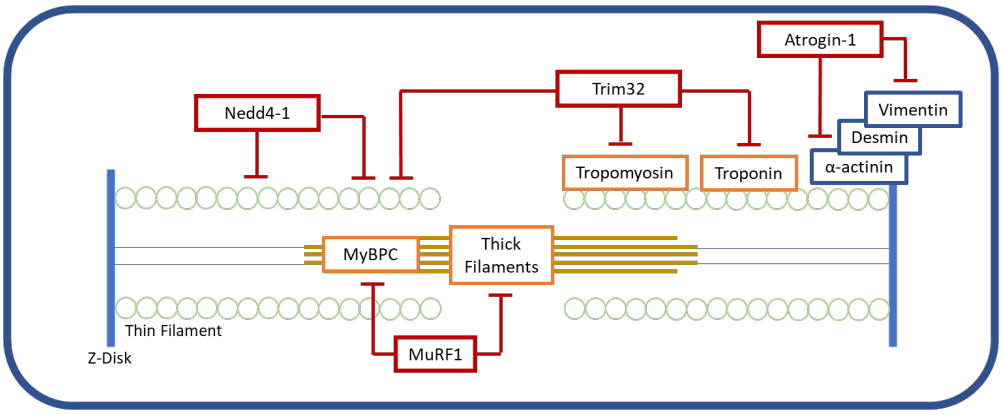

Figure 5: Sarcomeric targets of E3 ubiquitin ligases in skeletal muscle.

Although the exact role of myogenesis from satellite cells in protection against atrophy is unclear, it should be noted that E3 ligands target proteins involved in myogenesis as well as already-assembled sarcomeric proteins.[74] Thus, activation of the UPS may promote skeletal muscle atrophy both via degradation of existing myofibrils and the prevention of the inclusion of new myoblasts into the myofiber. Again, more research is needed to determine the significance of myogenesis in atrophy prevention.

Autophagy-Lysosome Pathway

Autophagosomes are membrane-bound vesicles containing damaged organelles, aggregated protein, and other cytosolic constituents in need of degradation. Two forms of autophagy via autophagosomes exist: basal and starvation-induced.[80, 89] Basal autopaghy involves the selective autophagic degradation of aggregated proteins and damaged

organelles or other cellular constituents, and is profoundly important for continued cell functioning and homeostasis. Starvation-induced autophagy occurs in times of nutrient depletion, and involves the non-specific degradation of cellular constituents for their use in cellular metabolism.[80] One of the first initiating steps in the formation of the autophagosome is activation of ULK1 and an associated complex of proteins. As mentioned above, ULK1 is phosphorylated by activated mTORC1, and therefore inhibited when mTORC1 is active in times of adequate nutrient supply.[80] In nutrient and amino acid depletion, mTORC1 is inhibited. An alternative pathway mediated by upregulation of AMPK in response to depletion of ATP levels is simultaneously upregulated, and both factors lead to increased ULK1 activation.[80] ULK1 and its protein complex then activate formation of a phagopore, an initially flat lipid membrane associated with a portion of the endoplasmic reticulum (ER) called an "omegasome." In specific conditions, additional lipids are added to the phagosome until it becomes curvilinear, then spherical, and encloses the structure(s) in need of degradation.[89, 90] The mechanisms by which the autophagosome "senses" what selected structures should be incorporated is currently unclear.[89] However, once the autophagosome has formed a complete sphere, it is transported to and fuses with a lysosome to carry out protein degradation.

Intracellular lysosomes are spherical, membrane-bound vesicles containing more than 50 types of proteases, lipases, glycosidases, nucleases, and phosphatases that degrade organelles and proteins.[80] They maintain an acidic intravesicular pH via membrane-bound proton vacuolar ATPases (V-ATPases); this acidic environment helps to optimize

the activity of the hydrolytic enzymes contained within.[80] The outer membrane of the mature autophagosome fuses with the lysosomal membrane, at which time the inner membrane of the autophagosome, as well as its contents, are hydrolyzed and degraded into their molecular constituents for recycling into new structures or use in metabolic pathways.[90]

Although both the UPP and starvation-induced ALP pathways contribute to myofiber atrophy, the UPP is more extensively studied. Inhibition of the ALP can lead to detrimental buildup to dysfunctional cellular components, so inhibition of the UPP as a clinical intervention to prevent cachexia is a more attractive option.[74]

Chapter 4: Regulation of Pro- and Anti-Atrophy Pathways in Chronic Kidney Disease

Multiple, diverse regulatory mechanisms determine the activity of the mTORC1, UPP and ALP pathways within any given cell, as well as the effect that chronic disease states might have on these pathways. A few of the ways that disease states can influence protein anabolism and catabolism are discussed below. When possible, the discussion will focus on chronic kidney disease, and applications to small animal medicine will be explored when available.

Insulin/IGF-1 Pathway in Disease

Metabolic acidosis is a known sequelae of CKD and the buildup of uremic toxins within the bloodstream. Acidosis can have an inhibitory effect on the insulin/IGF-1 pathway, and thus an inhibitory effect on Akt activation and mTORC1 signaling. In vitro, incubation of rat myotubes in pH 7.1 impaired PI3K signaling, a mediator in the insulin/IGF-1 pathway that is involved in the phosphorylation of Akt.

In addition to its effects on mTORC1 activation and muscle hypertrophy, phosphorylated Akt (pAkt) that results from IGF-1 receptor signaling also has downstream inhibitory effects on the UPP and apoptosis.[91] Specifically, pAkt phosphorylates forkhead box O (FOXO) proteins (FOXO1 and FOXO3), denying them access to the nucleus where they

activate transcription of atrophy-associated genes such as the E3 ubiquitin ligases MuRF-1 and atrogin-1.[92, 93] In addition, pAkt is inhibitory to caspase 3, a major regulator of cellular apoptosis.[91, 94] In one study, human subjects with CKD had a 40% decrease in Akt phosphorylation in skeletal muscle compared with control subjects, likely indicating that CKD reduces IGF-1/Akt signaling.[95] Mechanisms by which CKD may effect this decrease in pAkt are discussed in the next sections.

Myostatin & Activin A

Myostatin and activin A are two proteins in the transforming growth factor β (TGFβ) superfamily. Myostatin is almost exclusively are produced and released by myocytes.[96] Congenital mutations in myostatin resulting in its loss of function have been described in cattle, sheep, dogs, and humans; this mutation results in a phenotype with markedly increased muscle mass.[97-100] Both proteins bind activin receptors, which in turn activate signaling proteins SMAD2 and SMAD3, resulting in reduced phosphorylation and thus reduced activation of Akt.[101, 102] Recall from the previous section that Akt positively regulates mTORC1 to induce muscle protein synthesis. In addition to this effect, Akt negatively regulates transcription factors (forkhead box proteins) for muscle-specific E3 ubiquitin ligases MuRF-1 and atrogin-1.[101] Additionally, activation of the activin II B receptor (ActRIIB) leads to activation of p38β-MAPK, which upregulates the muscle-specific E3 ubiquitin ligase atrogin-1.[103] Thus, myostatin and activin A binding activin receptors causes increased protein degradation and decreased protein synthesis in skeletal muscle. In addition to their negative effects on skeletal muscle size, myostatin and activin

also induce skeletal muscle fibrosis in mice.[101, 104] Subtotally-nephrectomized mice developed increased collagen deposition in the tibialis anterior and gastrocnemius muscles in comparison to control mice, which was inhibited by decreasing myostatin signaling.[104]

A recent study of Japanese participants found a significant positive correlation between myostatin levels and decreases in kidney function as assessed by estimated glomerular filtration rate (eGFR) and estimated creatinine clearance (ClCr).[105] Similarly, muscle biopsies from human CKD patients undergoing dialysis catheter placement had increased myostatin and decreased myofiber size compared to controls.[91, 106] In mice, multiple studies have demonstrated an increase in muscle myostatin expression and a decrease in muscle weight in induced CKD; the decrease in muscle weight was at least partially ameliorated by inhibition of myostatin or its upstream stimuli.[106, 107] While it is unclear whether increased levels of myostatin in CKD are present due to decreased clearance or increased synthesis, it is known that CKD patients have increased markers of systemic inflammation.[106, 108] In particular, increased levels of the inflammatory cytokine IL-6 have been documented in mice with experimental CKD, resulting in downstream signaling through the JAK/STAT3 pathway that is associated with upregulation of myostatin.[106, 107] Interestingly, inhibition of myostatin signaling not only improved muscle condition in the mice, but also suppressed the production of inflammatory cytokines tumor necrosis factor (TNF)-α, IL-6, interferon (IFN)-γ, and macrophage colony-stimulating factor-1.[107] Activin A expression has also been associated with the production of pro-inflammatory cytokines.[109] This indicates that activin and myostatin

signaling are pro-inflammatory, and also result in a positive feedback that produces more myostatin and could interact with the nuclear factor (NF)-κβ pathway described below.

Investigation of the role of myostatin in canine and feline skeletal muscle has focused on Golden Retrievers with a model of Duchenne muscular dystrophy. One study investigating long-term myostatin inhibition in affected Golden Retrievers found increases in skeletal muscle weights from 27-49% after 13 months. The increases were mediated almost entirely by increased size of type IIA fibers, which may express more activin IIB receptors than type I myofibers.[110] A 20-25% reduction in skeletal muscle fibrosis was also noted, depending on the muscle tested.[110] Another study investigated UPP and myostatin proteins in dogs bred by cross-breeding Golden Retrievers with Duchenne muscular dystrophy with "Bully" whippets lacking functional myostatin, resulting in a Whippet with a "double-muscle" phenotype. Using only resulting progeny with Duchenne muscular dystrophy, but with decreased levels of functional myostatin, the study evaluated expression of genes involved in ubiquitination, protein quality control, and proteasomal activity. Interestingly, while the variability in expression of MuRF-1, atrogin-1, and many other genes involved in the UPP and protein regulation did increase, absolute decreases in expression of these genes did not occur in dogs with decreased myostatin activity.[111] Clinically, the cross-bred "GRippet" dogs in this study actually had a more severely affected skeletal muscle phenotype than their counterparts with Duchenne muscular dystrophy.[111] Another study using the GRippet crossbreed model found unequal muscle growth and increased joint contracture in GRippets compared to dogs with muscular dystrophy alone.[112] It is unclear whether this

contradictory finding results from differences in myostatin activity in dogs with muscular dystrophy or an idiosyncrasy of the GRippet model, but it does add some uncertainty as to the definitive role of myostatin in canine skeletal muscle.

Freeman et al recently performed a pilot study in six dogs with cachexia resulting from congestive heart failure (CHF), in which an injectable activin II B receptor decoy was used to achieve myostatin inhibition for four weeks.[113] At the end of the study period, median subjective muscle condition scores for the dogs had increased to a level which approached statistical significance ($p = 0.06$).[113] Assessing the changes noted in individual dogs, three showed apparent improvements in muscle condition, while three appeared unaffected.[113] As this was a pilot study with a small number of included dogs, further studies evaluating the study drug are intriguing; unfortunately, the study drug became unavailable shortly after the study was completed.[113] Further studies with larger numbers which differentiate between underlying global disease categories (cardiac, renal, neoplastic, etc.) as well as types of disease within these categories are warranted in future. Multiple myostatin and activin inhibitors are currently under investigation in human medicine, so additional studies using other pharmacologic agents may soon become feasible in cats and dogs.

NF-κβ & Pro-Inflammatory Cytokines

NF-κβ proteins are homo- or heterodimers that are ubiquitously expressed in almost every cell type and positively regulate gene transcription (with a few exceptions).[114] In

mouse models, transgenic mice exhibiting constitutive expression of NF-κβ developed smaller skeletal muscles and lower body weights than their wild-type counterparts, mediated at least in part by upregulation of MuRF1 ubiquitin ligase expression.[115] Recall from the previous section that MuRF-1 ubiquitinates, and therefore marks for proteasomal destruction, components of the sarcomere of skeletal muscle. In other studies, blockade of NF-κβ partially protected mice from cancer- or denervation-induced cachexia in the same study, and prolonged the survival of tumor-bearing mice.[115] Several other studies in mice have found a protective effect, especially on fast-type (type II) myofibers, of NF-κβ inhibition in atrophy induced by unloading or denervation.[116-118] Inhibition of NF- κβ also promoted satellite-cell-mediated regeneration of skeletal muscle tissue after induced damage in mice.[117, 119] However, when investigating age-related sarcopenia in mice with sustained inhibition of NF-κβ, skeletal muscle loss with age was worse in mice in which NF-κβ was inhibited.[120] This study also identified upregulation of several pro-atrophy pathways associated with the prolonged inhibition of NF-κβ, including myostatin activation, proteasome activity, transcription of several genes involved in the autophagy-lysosome pathway, and levels of IGF binding protein 5 (IGFBP5), which suppresses IGF-mediated muscle growth.[120] The reason for this conflicting finding is unclear, but these findings may indicate that different mechanisms are involved in regulation of age-related skeletal muscle atrophy compared to atrophy induced by disuse, denervation, or disease.[120]

NF-κβ has a variety of endogenous and exogenous stimuli, including bacterial and viral products (i.e. lipopolysaccharide, double-stranded RNA, etc.), angiotensin II, and

inflammatory cytokines TNF-α, IFN-γ, IL-1, and IL-2. Such stimuli cause degradation of endogenous inhibitors of NF-κβ (Iκβs), leading to its activation and entry into the nucleus, where it can regulate transcription of multiple genes.[121] The NF-κβ pathway is known to be upregulated in humans with CKD as a result of increased toll-like receptor (TLR), nod-like receptor (NLR), and angiotensin II activation of this pathway.[122] In a study of humans with CKD undergoing dialysis catheter placement, the rectus abdominus muscle expressed higher levels of TLR-4 (an activator of NF-κβ), and various downstream signals within the NF-κβ pathway, including MuRF-1, compared with muscle from control subjects.[95] Additionally, incubation of mouse myotubules with serum from uremic patients induced upregulation of phosphorylated p38-MAPK, a downstream marker of NF-κβ activation and an upregulator of atrogin-1.[95] Another study identified increased inflammatory cytokine levels, including TNF-α, in muscle biopsies from human patients with CKD compared to controls.[106] TNF-α mRNA was also increased in CKD patients in that study.[106] Thus, NF-κβ activation upregulates protein degradation and skeletal muscle mass decreases in disease states, and is activated by inflammatory and endocrine markers that are upregulated in CKD patients.

Another potent activator of NF-κβ signaling is a cytokine in the TNF superfamily, TNF-like weaker inducer of apoptosis, or TWEAK. NF-κβ activation can occur via two separate mechanisms, termed the “canonical” and “alternative” pathways. Both pathways lead to NF-κβ nuclear translocation and gene transcription.[123] TWEAK binding to its receptor, Fn14, can also upregulate p38-MAPK signaling.[124] TWEAK and the Fn14 receptor are both expressed in tubular and glomerular cells, and their expression increases

in multiple forms of CKD and AKI in humans.[124] In mice, increased levels of TWEAK led to reduced skeletal muscle fiber cross-sectional area and increased expression of atrogin-1 and MuRF-1.[123] In contrast to TNF- α, which causes a rapid, but transient, increase in NF-κβ via only the canonical pathway, TWEAK signaling causes slow, sustained NF-κβ activation via both canonical and alternative pathways.[123] TWEAK was also associated with a transition from slow, oxidative, type I muscle fibers to fast, glycolytic, type II fibers in mice, which are more vulnerable to atrophy than type I fibers.[123]

While no studies evaluating the NF-κβ pathway and PEW/cachexia in feline and canine CKD patients are currently available, feline and canine CKD have known associations with increased markers of systemic inflammation.[125, 126] If intracellular signaling pathways downstream of these inflammatory markers are similar in dogs and cats to those in human patients and mice, systemic inflammation secondary to CKD (or the decreased clearance of inflammatory mediators as GFR declines) could lead to NF-κβ- and myostatin-induced skeletal muscle atrophy. However, further studies are needed in dogs and cats to better elucidate this relationship.

Glucocorticoids

Glucocorticoids (GCs) are secreted by the zona fasciculata of the adrenal gland in response to pituitary adrenocorticotrophic hormone (ACTH), and the many actions of glucocorticoid hormones are essential for life, such as supporting vascular tone and

glucose homeostasis.[127] Glucocorticoid secretion can be increased by physiologic stress, including chronic disease.[128] Metabolic acidosis, such as that observed in CKD, can also lead to glucocorticoid production, and glucocorticoids may be necessary for acidosis-mediated weight loss.[56, 129] In skeletal muscle, GCs promote protein catabolism to increase circulating free amino acid concentrations for use in gluconeogenesis.[128] Acutely, this has the beneficial effect of supporting blood glucose levels and tissue ATP production.[128] With chronic elevation of GCs, however, the detrimental effects of skeletal muscle mass and function loss and insulin resistance outweigh these benefits.

GCs have known insulin-antagonizing effects, and increased circulating levels of GCs can decrease Akt phosphorylation by insulin and IGF-1, leading to downregulation of mTORC1 and decreased protein synthesis.[128] IGF-1 synthesis in muscle may also decrease in response to GCs, as does expression of insulin/IGF receptor substrates.[128] Moreover, in the fasted state, increased UPP degradation as a result of upregulation of MuRF-1 has been demonstrated with exogenous GC treatment.[128] Upregulation of mediators of the myostatin pathway also occurs with GC treatment in mice.[106, 128] Lastly, GC administration can also decrease blood flow to skeletal muscle beds.[128]

GC levels have a weak, but negative and significant correlation with eGFR in human patients with CKD and hypertension, and negative feedback mechanisms within the hypothalamic-pituitary-adrenal axis may also be disrupted in patients with CKD.[130, 131] GC secretion in dogs and cats with CKD has not been evaluated, but is another potential contributing factor to the development of cachexia seen in these patients and warrants further investigation.

Angiotensin II

The effects of the renin-angiotensin-aldosterone (RAAS) system, and the systemic effects of angiotensin II (ATII) are well-described elsewhere. Briefly, in response to perceived hypovolemia, the juxtaglomerular apparatus of the kidney secretes renin into circulation. Renin acts on angiotensinogen from the liver, converting it to angiotensin I. Angiotensin converting enzyme (ACE), located mainly in the lungs, converts angiotensin I to ATII, which exerts effects on multiple body systems, including vasoconstriction, adrenal aldosterone secretion, antidiuretic hormone release, thirst, and renal sodium retention.[132]

More recently, local, atrophic effects of ATII on skeletal muscle have also been described, despite the fact that ATII receptor expression in mouse and rat skeletal muscle is nonexsistent.[94, 133] In rats and mice, infusion of ATII resulted in decreased muscle weights, increased proteasomal protein degradation, and increased synthesis of MuRF-1 and atrogin-1 compared to controls.[94, 133-136] ATII-mediated atrophy was most prominent in type IIB fibers.[133] Subsequent studies determined that ATII-mediated increases in atrogin-1 expression in skeletal muscle occurred secondary to reduced pAkt and increased FOXO transcription.[133-135, 137] Increases in apoptotic signals were also observed in ATII-infused mice, secondary to reduced pAkt signaling, suggesting that ATII results in disruption IGF-1 signaling in skeletal muscle.[94, 133, 138] MuRF-1 expression increased in response to ATII infusion as well, but this increase appeared to be independent of Akt and may be mediated by ATII-dependent upregulation of an additional transcription

factor, TFEB, which was shown to mediate ATII and starvation induction of MuRF transcription in mouse myotubes.[134, 135, 139 140]

Interestingly, the ability of ATII to induce skeletal muscle atrophy was attenuated by glucocorticoid inhibition in one study, indicating possible dependence of ATII-mediated skeletal muscle wasting on glucocorticoid upregulation.[94] IL-6, in concert with serum amyloid A (SAA) was also necessary for ATII-induced atrophy, and IL-6 and SAA synthesis were in turn induced by ATII signaling.[133] Thus, increased circulating ATII levels may induce skeletal muscle wasting by decreasing IGF-1/Akt, as well as inducing inflammatory cytokines which upregulate myostatin and NF-κβ signaling. Indeed, a recent study identified increased myostatin mRNA levels in mouse myotubes stimulated by ATII.[138]

In addition to the effects described above, ATII may also mediate skeletal muscle atrophy via the induction of mitochondrial dysfunction and reactive oxygen species (ROS) production.[138, 139] In a recent study in mice by Liu et al, ATII infusion not only induced production of MuRF-1, atrogin-1, and myostatin *in vivo*, but also increased markers of ROS production and mitochondrial dysfunction in mouse myotubes.[138] Additionally, ATII production led to upregulation of proteins associated with the NLRP3 inflammasome, a multi-protein complex that activates inflammation via caspase 1 activation and cleavage of IL-1β and IL-18 to their active forms. NF-κβ signaling also upregulates transcription of genes encoding inflammasome components.[141] Knockout of the gene encoding the NLRP3 component of the inflammasome, as well as treatment of

myotubes with a mitochondrial antioxidant (Mito-TEMPO) attenuated the ATII-dependent increases in myostatin and E3 ubiquitin ligases, ROS production, and markers of mitochondrial dysfunction, and also reduced ATII-induced skeletal muscle loss.[138] Treatment of the mice with the PPAR-γ receptor agonist, rosiglitazone, also attenuated the ATII-induced changes.[138] Another study also found upregulation of ROS after ATII infusion, and identified an upregulation in the activity of NADPH oxidase, an enzyme found in the plasma membrane and lysosomes which produces ROS to kill invading pathogenic organisms., The increased NADPH oxidase activity then led to ROS production and subsequent skeletal muscle atrophy in response to stimulation of the ATII receptor.[142]

Counterintuitively, ATII's disruption of mitochondrial function may result from dysregulation and inhibition of the autophagy-lysosome pathway (ALP). Another recent study found that *in vivo* ATII infusion in mice disrupted formation of the autophagosome, which resulted in accumulation of swollen, disorganized mitochondria within the mouse myocytes.[136] Supporting this finding, oxidative respiratory capacity was reduced in skeletal muscle infused with ATII, as was activity of the PCG-1α, a gene which upregulates mitochondrial activity.[136] Interestingly, this study also found increased activation of downstream components of mTORC1 in response to ATII infusion, indicating that increased mTORC1 signaling may be responsible for inhibiting autophagosome formation in this setting.[136] Since other studies have associated ATII with decreased IGF-1/Akt activation, the upstream activators of mTORC1 activity, it is

unclear how ATII downregulates IGF-1 but upregulates mTORC1 simultaneously, especially in the absence of its own skeletal muscle receptor.

In addition to promoting cellular pathways involved in skeletal muscle wasting, ATII infusion also decreases appetite in mouse models.[134, 136] While an in-depth discussion of appetite regulation is beyond the scope of this paper, many diseases in which muscle catabolism is a clinical feature also lead to anorexia/hyporexia. Decreased caloric intake in response to increased ATII levels, in addition to the metabolic alterations described above, contributes to a state of stressed starvation, subsequently speeding the development of cachexia.

In human CKD patients receiving chronic dialysis, ATII receptor antagonist administration decreased the odds of developing reduced handgrip strength by 75%.[143] ATII's effects on skeletal muscle homeostasis in cats and dogs have not been studied. However, plasma renin activity, angiotensin I, ATII, and aldosterone concentrations have been shown to be increased in cats with naturally-occurring CKD compared to controls.[144] Experimental induction of CKD in dogs also produced significant increases in plasma renin activity, angiotensin I, ATII, and aldosterone concentrations.[145] As such, investigation of the effects of ATII antagonism in skeletal muscle preservation for canine and feline CKD patients is an intriguing possibility for future research studies.

It should be noted that most of the regulatory pathways discussed above also have deleterious effects on satellite cell activation, myoblast differentiation, and skeletal muscle hyperplasia. However, given that the role of hyperplasia in muscle hypertrophy and protection against atrophy is currently unclear, an in-depth discussion of these pathways' effects on satellite cells is beyond the scope of this paper.

Chapter 5: Quantification of Skeletal Muscle in Human and Animal Medicine

The study and management of cachexia in human, canine, and feline patients demand methods to quantify body muscle mass that are non-invasive, inexpensive, and readily accessible. The nutritional assessment scoring systems discussed in the first chapter all incorporate some measure of muscle mass or function for human patients, such as DEXA, MRI methods, gait speed and grip strength measurements, and others. While some of the tools used in human medicine to help identify subtle losses of muscle mass and strength might apply to veterinary medicine, others translate poorly to use in dogs and cats. The next section details some of the modalities used to quantify muscle mass and quality in human patients, as well as available information on their use in veterinary medicine.

Dual X-Ray Absorptiometry (DEXA)

Attenuation of an x-ray beam through a given tissue depends on the energy contained within that beam. In DEXA, two x-ray beams of different energies are passed through a test subject, and based on the attenuation of those beams, the proportion of the subject that is comprised of bone, fat mass, and FFM can be calculated.[146] In humans, DEXA

assessment of appendicular skeletal muscle mass is a component of multiple definitions of sarcopenia and cachexia (see Chapter 1).

DEXA is currently regarded as the gold standard for body composition analysis in human medicine.[147] However, differentiation between fat mass and FFM requires the use of mathematical equations which assume that hydration of FFM remains constant at 73%.[148] This assumption means that DEXA skeletal muscle mass calculations are dependent on constant skeletal muscle hydration. Thus, disease processes that affect fluid distribution (CKD, CHF, liver failure), dehydration, as well as age-related changes to fluid distribution will affect muscle mass estimates.[147] Note also that FFM includes skeletal muscle and organ masses (but not bone), so significant changes in organ volumes with disease may change the percentage of FFM comprised by skeletal muscle.[149] DEXA scan results and calculations for fat mass vs. FFM are subject to inter-rater variability as well as position-dependent variability.[150] Newer, fan-beam scanners may reduce scan times to 5-6 minutes; historically, scan times could take up to 20 minutes .[146, 150] With shorter scan times, it is possible that DEXA analysis under short sedation may become more clinically attractive; however, few veterinary institutions have DEXA scanning available on-site. Thus, availability remains a significant barrier to its use.

DEXA-predicted body weight in healthy cats correlated well with measured body weight, and measures of fat mass and FFM were repeatable between different scans of the same animal in both cats and dogs.[151] Another study evaluating both dogs and cats compared DEXA-derived FFM measures to post-mortem chemical analysis, and found good

agreement across individuals.[152] However, when assessing individual animals, large discrepancies (up to 13.22%) between DEXA estimates and results from chemical analyses were noted in individuals with high fat content in their skeletal muscle, or high water content in their mesenteric fat.[152] Adding water to samples of lean beef prior to DEXA analysis also caused the machine to "over-estimate" the fat content of the lean beef sample, indicating that changes in patient body water content will affect fat mass to FFM proportions.[152] Another study in healthy dogs, DEXA mean estimates of FFM percentage differed by 10% from FFM percentage via chemical analysis, although this difference was not statistically significant.[149] Yet another study found that DEXA underestimated FFM in healthy dogs by a mean of 7.3% compared to deuterium oxide dilution methods (a method used in research settings which also estimates total body water and calculates FFM based on muscle hydration assumptions).[153] No evaluation of DEXA's accuracy has been performed in cats and dogs with differing hydration or disease status. As such, it is currently unclear whether application of DEXA to ill animals with significant cachexia, for research purposes or clinical assessment, will be reliable.

Bioimpedance Analysis

Bioimpedance analysis (BIA) relies on inherent obstruction of electrical current flow in bodily tissues to determine body composition. Briefly, electrical current flow is "impeded" by both low-water and electrolyte-containing tissues (termed resistance) and by lipid cell membranes (termed reactance). If you run an electric current through a group of tissues, the total impedance to that current will be the sum of the resistances from

high-resistance (skin, fat, bone) and low-resistance (skeletal muscle, fluid) tissues, and impedance from lipid membranes. “Alternating currents” are electrical currents that flow back and forth a specific number of times per second (i.e. at a specific frequency). Using alternating currents of different frequencies through a given group of tissues will produce different amounts of resistance and reactance through those tissues. At low frequencies, reactance is approximately zero, and all the impedance to current flow comes from resistance from tissues. Reactance rises as the frequency of the alternating current increases; equations exist that calculate the proportion of high- and low-resistance tissues that correspond to specific patterns of reactance and resistance changes as the current frequency changes.[146]

BIA is relatively inexpensive, non-invasive, and can be performed quickly in an awake animal. However, like DEXA, BIA is altered with changes in hydration status, age, edema, and obesity, decreasing its utility in patients with disease; BIA also assumes a constant skeletal muscle hydration of 73% for its calculations to be correct.[146, 154, 155] In a study in cancer patients comparing BIA with DEXA and CT estimates of total body skeletal muscle mass, BIA results agreed only poorly with DEXA.[30] In dogs, FFM estimation by single-frequency BIA correlated fairly with DEXA, but limits of agreement were clinically unacceptable.[148] However, another study using multi-frequency BIA in healthy, lean dogs found better correlation with DEXA and tighter limits of agreement in FFM measures.[154] In a population of mostly-healthy, non-obese cats, single-frequency BIA in combination with zoomorphic measurements (such as forelimb circumference) measured FFM with good correlation to proximate analysis; however, no studies have

been performed in cachectic, obese, or ill cats.[155] Further studies are warranted in evaluating the accuracy of BIA in predicting FFM in disease states, and in monitoring changes in FFM through time in dogs and cats.

Ultrasonography

The use of ultrasound to evaluate muscle thickness, volume, or cross-sectional area as a predictor of total body skeletal muscle mass has been described in human patients. A study in women found that a combination of ultrasound-determined thicknesses of multiple muscle groups, in combination with BMI and age, was highly correlated with DEXA-assessed appendicular lean body mass.[25] In older patients, studies have shown good agreement with DEXA using combinations of thigh and arm or thigh and lower leg muscle thicknesses.[31] Adults enrolled in this study suffered from chronic obstructive pulmonary disorder, coronary artery disease, and stroke, indicating that ultrasound may have utility in diseased patients at risk for cachexia development.[31] In adults with non-dialysis-dependent CKD, ultrasound-determined cross-sectional area of the rectus femoris muscle was correlated with physical performance, as well as thigh muscle skeletal volume measured on MRI.[156] Additionally, both MRI of the thigh and ultrasound of the rectus femoris were able to detect increases in muscle area or volume after 12 weeks in an exercise program.[156] Furthermore, most studies evaluating ultrasound in assessment of skeletal muscle in older human patients have shown good intra- and inter-rater reliability for the measurement as well, even in studies where inexperienced operators were compared to those with experience.[31, 35] Keep in mind, however, that the

muscle groups generally evaluated in humans are much larger than typical muscle groups in canine and feline patients, so these results may not translate to the veterinary setting. Ultrasound techniques are also currently being developed that use the echogenicity or elastography to assess muscle quality; no studies evaluating echogenicity or elastography are currently available in veterinary medicine.[157]

In dogs with varying diseases, ultrasound of the epaxial musculature height at the level of T13, normalized to body size by dividing out the length of T4 as assessed on a thoracic radiograph, correlates to subjective muscle condition scores.[52] This measure is titled the "VEMS"; a "FLEMS" normalized to forelimb circumference, also correlates to muscle condition scores, although the coefficient is lower.[52] Both the VEMS and FLEMS correlated, albeit poorly, to quantitative magnetic resonance measures of lean body mass (discussed below).[52] A similar study evaluating the VEMS in healthy Golden Retrievers found that it successfully identified a lower muscle mass in older vs. younger study participants. Temporal and quadriceps muscle thickness were not affected by age.[158] Additionally, the VEMS intra- and inter-rater reliability was assessed in a separate study, which found good intraclass correlations between VEMs performed by different observers (0.8-0.99).[159] It is worth mentioning, however, that on an individual basis, the VEMS differed between observers by as much as 25% of the mean VEMS value on Bland-Altman analysis.[159]

The VEMS was also evaluated in 29 healthy cats; no differences between male and female cats were noted, and the VEMS calculation was not statistically different

regardless of whether the cat was standing or crouching for the ultrasound.[160] However, evaluation of the VEMS in comparison to a measure of skeletal muscle or lean body mass has not been performed in cats. Further studies in dogs and cats with specific disease states, compared to gold-standard measures of skeletal muscle mass (such as they are) are certainly warranted, as ultrasound could provide an inexpensive, non-invasive estimate of skeletal muscle mass in awake animals.

Magnetic Resonance

Magnetic resonance principles rely on the abundant water molecules, and the hydrogen atoms they contain, to distinguish types and locations of tissues within a magnetic field. The human body, as well as the bodies of companion animals, are approximately 2/3 water. Each water molecule contains two hydrogen atoms. All atoms, including the hydrogen atoms in body water, have an inherent angular momentum, termed "spin". In a magnetic field, a majority of these angular momentum vectors will align themselves with the direction of the field. If the magnetic field is then perturbed, the spins will be "knocked" out of alignment with the magnetic field vector, then return to place over time. The atom type and its chemical bonding will affect how this realignment occurs, and the magnetic field itself can be manipulated so that atoms in different regions will realign slightly differently. This allows for differentiation of the location and types of hydrogen-containing tissues within the body. Computer software can resolve these multiple spin realignments into an image (magnetic resonance imaging, MRI) or can be used to gain insight into the relative percentage of the body composed of different tissue types

(quantitative magnetic resonance, QMR). The difference between MRI and QMR is that in QMR, the signal is obtained from the whole body at once and differentiates the strength of signal from hydrogen ions in adipose tissue and fat-free tissue, without using complex manipulation of the magnetic field to "code" the actual spatial location of each hydrogen atom.[161] As a result, QMR is much faster (1-4 minutes), and requires less training to perform than traditional MRI.[161]

MRI is very sensitive for differentiation of skeletal muscle from adipose tissue, skin, and organ soft tissues; quantification of skeletal muscle within the MRI image can be performed with commercially available software.[157] Many studies use MRI rather than DEXA as the reference standard for skeletal muscle quantification.[157] In humans, good correlation exists between the skeletal muscle present in a single cross-sectional abdominal MRI image and total body skeletal muscle volume.[33, 34] Using a single transverse image, cross-sectional area can be calculated for all skeletal muscle present in the image, or single muscle groups can also be singled out for measurement.[29, 33, 34] In particular, cross-sectional areas of the mid-thigh and psoas muscle groups were correlated to FFM assessed by DEXA.[29] Estimation from a single slice saves time and cost over attempting to quantify skeletal muscle throughout the body entire.[34] In addition, modifications to the MRI protocol can also aid in assessing muscle for infiltration of non-contractile elements, like fibrosis or adipose tissue infiltration.[157]

In Beagles, validation studies on QMR have been performed, comparing QMR to DEXA and deuterium oxide dilution tests (D_2O).[153] While QMR, DEXA, and D_2O measures of

lean body mass were highly correlated, QMR underestimated D_2O-determined FFM by 13.4%, and this negative bias increased with increasing FFM.[153] However, the coefficient of variation between QMR studies performed on the same animal was < 2% except in very lean animals, indicating that QMR might be useful if performed longitudinally in the same animal.[153] Interestingly, the hydration constant of FFM as calculated by QMR often differed by as much as 5% from the assumed constant of 73%, especially in leaner dogs.[153] It is unclear whether this represents error in the QMR technique, or whether this illustrates variation in muscle/organ hydration that might invalidate methods that rely on the assumption of constant skeletal muscle hydration (DEXA, BIA, D_2O). In cats, QMR underestimated lean body mass by only 4.4% compared to D_2O, outperforming DEXA (9.2% underestimation which was statistically significant).[162]

While QMR scanning is fast, requires none or minimal sedation depending on available restraint devices, and may be acceptably accurate in determining FFM, the limited availability of QMR scanners makes this technique most useful in the research setting. Traditional MRI is not generally used in animals for skeletal muscle quantification due to cost, time required for large-volume scanning, and general anesthesia requirements. However, many of the estimates of skeletal muscle quantity from a single, cross-sectional MRI image have been extrapolated to use with transverse CT images, which can be obtained faster and more cheaply.

Computed Tomography (CT)

CT scanning uses x-ray beams in a 360º configuration to provide a full-volume image of a subject, which can be analyzed slice-by-slice in the sagittal, transverse, or dorsal planes. Unlike DEXA, QMR, and BIA, CT (and MRI) imaging can differentiate lean body mass contained in skeletal muscle from that contained in organ tissues, an important consideration for skeletal muscle mass assessment in patients that may have growing neoplastic tumors. CT allows for high-resolution distinction between organs, skeletal muscle, and adipose tissue, on the basis of the Hounsfield unit ranges which correspond to the attenuation of the x-ray beam by each tissue type.[147] Hounsfield units from -29 to 150 correspond to skeletal muscle, and fat infiltration into muscle is linearly correlated with its CT attenuation.[21, 30] In humans, CT scans of the thigh and trunk have been used to calculate muscle cross-sectional area from a single slice, or muscle volume from a series of slices.[21]

Total body skeletal muscle quantity estimates from a single, cross-sectional CT slice are also possible, similarly to MRI.[28] In the study in cancer patients referenced in the BIA section, single-slice transverse CT estimates of skeletal muscle mass correlated well with appendicular and whole-body skeletal muscle measurements by DEXA.[30] The MRI-determined psoas cross-sectional area correlation with DEXA has also been extrapolated to use with CT images. As discussed in the first chapter, multiple CT-based definitions of sarcopenia have been proposed in the literature, using either normalized psoas muscle

cross-sectional area or total skeletal muscle cross sectional area at the level of L3 as a surrogate for total body skeletal mass.[22, 26]

In veterinary patients, performing a CT scan solely to quantify muscle mass is expensive and impractical. However, CT scan is commonly used in routine workup for disease processes like neoplasia that may increase the risk for development of cachexia. Currently, CT scan data is not used to comment on muscle mass and quality in canine and feline patients; however, every CT scan performed contains a wealth of information about that patient's body composition. If this information could be used to identify patients already in a "pre-cachectic" or PEW state, early intervention to prevent progression to cachexia could improve quantity and quality of life for these patients.

Studies evaluating CT for skeletal muscle assessment in dogs have already been performed. Recently, a study in healthy client-owned, sedated dogs compared skeletal muscle volume within the abdominal cavity (calculated by automated software with manual adjustments) to DEXA-assessed FFM. A strong correlation was identified between CT abdominal skeletal muscle volume and DEXA-determined FFM in that study.[163] Fat mass and bone mineral content were also strongly correlated to DEXA measurements, and inter- and intra-rater reliability of the CT measurement for fat mass were high.[163] Again, however, individual values could vary by as much as 45% between CT-predicted total FFM and DEXA-measured fat free mass, and agreement was worst in the smallest animals in the study.[163] The study authors believe this increase in variability is due to the use of an adult human DEXA software program that was less accurate in

very small patients.[163] Another study found that cross-sectional area of the epaxial musculature, normalized by dividing by the height of the vertebral body of T13, was significantly smaller in older Golden Retrievers compared to younger ones.[158] A sister study in the same population of dogs also found that mean attenuation values in the epaxial muscles on CT scan were lower in older dogs than in younger dogs, implying greater infiltration with adipose tissue in older Golden Retrievers.[164]

Prior to our study, no studies had evaluated the use of CT for assessing body composition in cats. Details of this study are described in the next chapter.

Chapter 6: Intra- and Inter-Rater Reliability in the Cross-Sectional Area of Feline Epaxial Musculature on CT Scan

Materials and Methods

Case Inclusion

Medical records from the Ohio State University Veterinary Medical Center from January 2005 to November 2017 were scanned for feline patients undergoing thoracic or abdominal CT as a part of routine diagnostic work-up. Cases with diseases associated with cachexia (CKD, neoplasia, cardiac disease, etc) were included, while cases in which focal pathology existed at the level of T13 were excluded. Cases were also excluded if the cat was <1 year old, if the CT image quality was too poor for reasonable assessment of the epaxial musculature, if the image did not include the entirety of the T13–L1 junction, if the cat had a transitional T13 or L1 vertebra, or if the cat was poorly positioned or was not in sternal recumbency for the CT scan. If a cat had more than one CT scan performed, only the first scan was included in the analysis. Data retained from the medical record included signalment, date of birth, date of CT scan, CT scanner used, the reason the CT scan was performed, body weight (BW), muscle condition score (MCS), body condition score (BCS), final diagnosis and comorbid conditions. BCS was recorded in the medical record based on a 5-point or 9-point scale at the discretion of the

attending clinician. For statistical analysis, values using the 5-point scale were converted to the 9-point scale as follows: 1/5 = 1/9; 1.5/5 = 2/9; 2/5 = 3/9; 2.5/5 = 4/9; 3/5 = 5/9; 3.5/5 = 6/9; 4/5 = 7/9; 4.5/5 = 8/9; 5/5 = 9/9. This conversion scale was utilized after consultation with a board-certified veterinary nutritionist (VP), as no authoritative protocol exists for conversion of BCS from a 5- to 9-point scale. Muscle wasting was categorized by severity and assigned an MCS as follows: none (0), mild (1), moderate (2) or severe (3).

When possible, the primary diagnosis and comorbid conditions for each cat were recorded. Primary diagnosis was assigned to the disease process that prompted the CT scan; comorbid conditions were defined as chronic conditions that preceded the CT scan visit, or conditions identified at the CT scan but unrelated to the primary active condition. Cats with pulmonary nodules identified on the CT scan were classified as having pulmonary neoplasia if no primary tumor was identified.

Epaxial Muscle Measurements

Transverse CT images for each cat were windowed and leveled to a standard value (W2500, L480) (E-Film 3.3; Merge Healthcare). Each image was then magnified 2.5 times. A slice including the body wall, right and left epaxial muscle groups, mid-body T13 vertebra, and the heads of the right and left 13th ribs was identified, and the image was centered on the body of T13, preventing visualization of the abdominal organs. A 1 cm calibration line was added to each image, and the image was then copied into ImageJ

software (National Institutes of Health) for further evaluation. A representative image after final processing is shown in Figure 6.

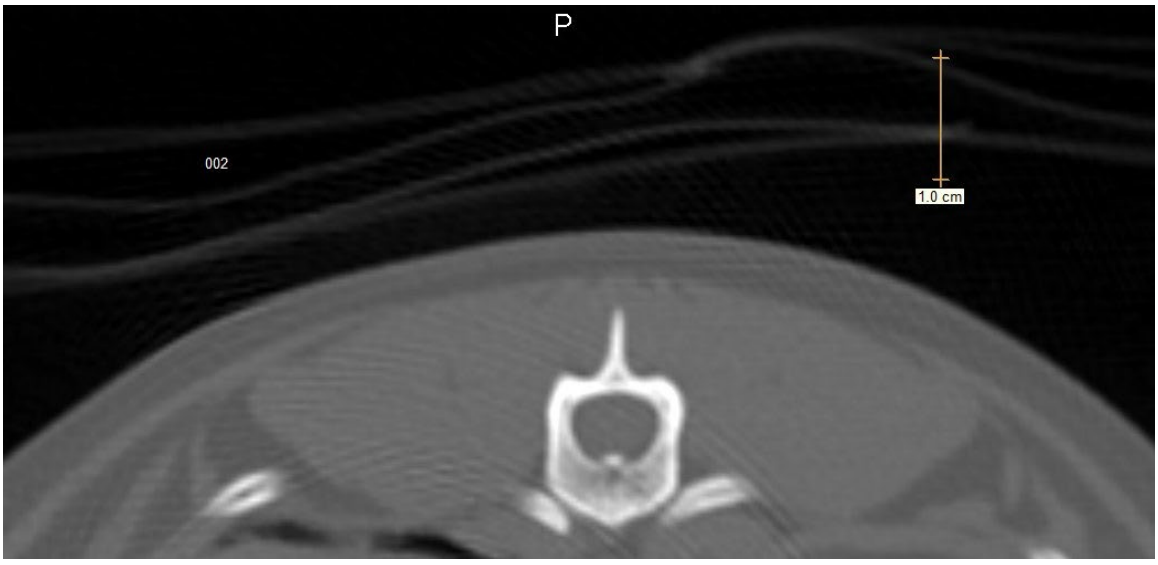

Figure 6: Representative CT image of feline epaxial musculature after processing for measurement.

In ImageJ software, the 1 cm line was measured, and the measurement was calibrated to correlate image pixels with length in cm for each image. The height of the T13 vertebral body was measured three times, and the result was recorded in centimeters. The right and left epaxial muscle groups were then outlined freehand by three observers: a board-certified radiologist (EG); a board-certified internist (JQ); and a resident in the internal medicine program at the Ohio State University Veterinary Medical Center (LR). Observers were blinded to each cat's signalment, diagnosis, BCS, MCS and other medical record data. After the right or left epaxial muscle group was outlined, the area (in cm^2) was calculated using ImageJ software, and this value was recorded. This

measurement was repeated three times for the right and left epaxial muscle groups, alternating which side was measured first. All measurements were repeated a second time by each of the three observers, at least 1 month after the first set of measurements was completed. Figure 7 demonstrates the measurements performed in ImageJ for each of the 101 included scans.

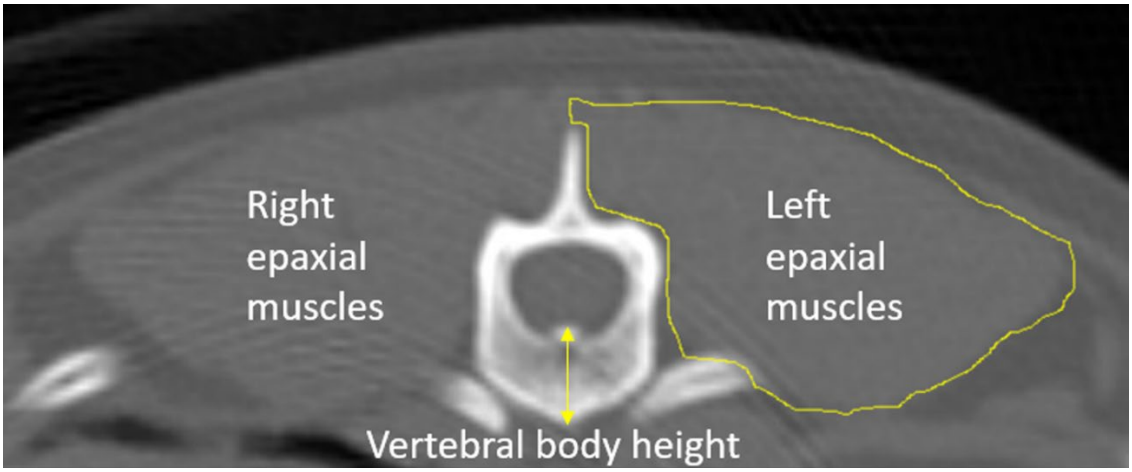

Figure 7: Measurements performed for each CT image.

Mean values for left epaxial cross-sectional area, right epaxial cross-sectional area and T13 mid-body vertebral height were calculated from the average of the three measurements for each. The average of the mean left and right cross-sectional areas was also calculated to give an overall epaxial cross-sectional area for each cat. Values for the mean right, left and overall epaxial cross-sectional areas were then divided by the mean midbody vertebral height to provide the left (LEMA), right (REMA) and average overall epaxial area:vertebral height ratios (EMA), to normalize this value for the overall size of the cat. Equations for calculating the LEMA, REMA, and EMA are as follows:

$$\text{REMA} = \frac{\text{average of three measurements of left epaxial group cross-sectional area}}{\text{average of three vertebral body height measurements}}$$

$$\text{LEMA} = \frac{\text{average of three measurements of right epaxial group cross-sectional area}}{\text{average of three vertebral body height measurements}}$$

$$\text{EMA} = \frac{\text{average left and right epaxial group cross-sectional area}}{\text{average of three vertebral body height measurements}}$$

Figure 8: Equations for REMA, LEMA, and EMA based on epaxial measurements for each CT scan.

Statistics

Descriptive statistics, such as mean and SD for continuous variables, and count and percentage for categorical variables, were provided. Intra-rater reliability was assessed for each observer with concordance correlation coefficients (CCC). The average measurements of the REMA, LEMA and EMA across time points for each observer were calculated, and inter-rater reliability of the average values were also assessed via CCC. Bland–Altman plots were generated to assess bias and limits of agreement (LoA) for the REMA, LEMA and EMA between observers and within observers. In the subset of cats with recorded MCS, median overall EMAs were compared between the four MCS groups using the Kruskal–Wallis test, with pairwise comparisons between MCS groups performed with Wilcoxon rank-sum test at a significance level of 0.0083 (0.05/6 comparisons) with Bonferroni correction for multiple comparisons. P values <0.05 were considered significant. All analyses were performed in Stata version 15.1 (Stata Corp).

Results

Review of the medical records identified 167 feline abdominal and thoracic CT scans. Of these, 62 were excluded according to the criteria described above. Four cats had more than one CT scan performed and only the first scan was included. In total, 101 feline CT scans from three CT scanners (Revolution EVO [GE Healthcare]; PQS [Picker Corporation]; LightSpeed Ultra [GE Healthcare]) remained in the final analysis; 21 were abdominal and 80 were thoracic scans. Of these, MCS was commented on in the medical records of 29 cats. Signalment and body composition characteristics of 101 included cats are presented in Table 3.

Table 3: Signalment and Body Characteristics of Included Cats. Descriptive Statistics are Median (Min, Max) or N (%) of Cats.

	All included cats (*n = 101*)	**Cats with known muscle condition** (*n = 29*)
Age, y	10.9 (1.68, 19.3)	11.02 (3.31, 19.3)
Weight, kg	4.85 (2.24, 11.8)	4.6 (2.52, 11.8)
Cats with value missing	*n = 5*	---
Body Condition Score	6 (1, 9)	6 (1, 9)
Cats with value missing	*n = 43*	*n = 3*
Muscle Condition Score	1 (0, 3)	1 (0, 3)
Cats with value missing	*n = 68*	---
Sex		
FI	4 (4%)	2 (6%)
FS	41 (41%)	14 (42%)
MC	54 (54%)	17 (52%)
MI	1 (1%)	0 (0)
Cats with value missing	*n = 1*	---

FI =female intact; FS =female spayed; MC =male castrated; MI =male intact

Breeds included domestic shorthair (n = 61), domestic longhair (n = 12), domestic mediumhair (n = 8), Maine Coon (n = 4), American Shorthair (n = 3), Abyssinian (n = 2), Persian (n = 2), Siamese (n = 2) and one each of six other breeds (Exotic Shorthair, Ragdoll, Japanese Bobtail, Himalayan, domestic longhair–Bengal cross and unspecified mixed breed). Breed information was not recorded for one cat.

Out of 58 cats, one had a BCS of 1/9, 2/58 had a BCS of 2/9, 11/58 had a BCS of 3/9, 7/58 had a BCS of 4/9, 14/58 had a BCS of 5/9, 4/58 cats had a BCS of 6/9, 15/58 had a BCS of 7/9, 0/58 had a BCS of 8/9, and 4/58 had a BCS of 9/9. Of the 29 cats with

muscle condition information available, 14 were classified as having normal muscling, six as having mild, five as having moderate and four as having severe atrophy. Intra-rater reliability of the epaxial muscle measurements is summarized in Table 4.

Table 4: Intra-Rater Reliability Assessed by Concordance Correlation Coefficient (CCC) (95% CI) and Bias (95% Limits of Agreement (LoA)).

Rater	REMA		LEMA		EMA	
	CCC (95% CI)	*Bias (95% LoA)*	*CCC (95% CI)*	*Bias (95% LoA)*	*CCC (95% CI)*	*Bias (95% LoA)*
EG	0.90 (0.86-0.94)	0.08 (-0.87, 1.04)	0.84 (0.78-0.90)	-0.16 (-1.38, 1.05)	0.90 (0.86-0.94)	-0.04 (-1.01, 0.93)
JQ	0.97 (0.95-0.98)	-0.08 (-0.71, 0.55)	0.97 (0.96-0.98)	-0.10 (-0.65, 0.45)	0.97 (0.96-0.98)	-0.09 (-0.65, 0.47)
LR	0.98 (0.98-0.99)	0.05 (-0.35, 0.45)	0.99 (0.98-0.99)	0.02 (-0.34, 0.38)	0.99 (0.99-0.99)	0.04 (-0.29, 0.36)
N = 101 feline CT scans						

CCCs between first and second epaxial measurements for all observers for REMA, LEMA and EMA ranged from 0.84 to 0.99. Agreements for measurement of the REMA and LEMA were similar across observers, indicating little to no effect of the side of the epaxial musculature measured on measurement agreement. However, for observers LHR and JMQ, the averaged value of both sides (EMA) showed better agreement between time points than the REMA or LEMA. For observer EG, the EMA showed equal agreement to the REMA and better agreement than the LEMA. For these reasons, the EMA was used for Bland–Altman analysis. Bland–Altman analyses of the measured EMA for each observer at both time points are presented in Figure 9.

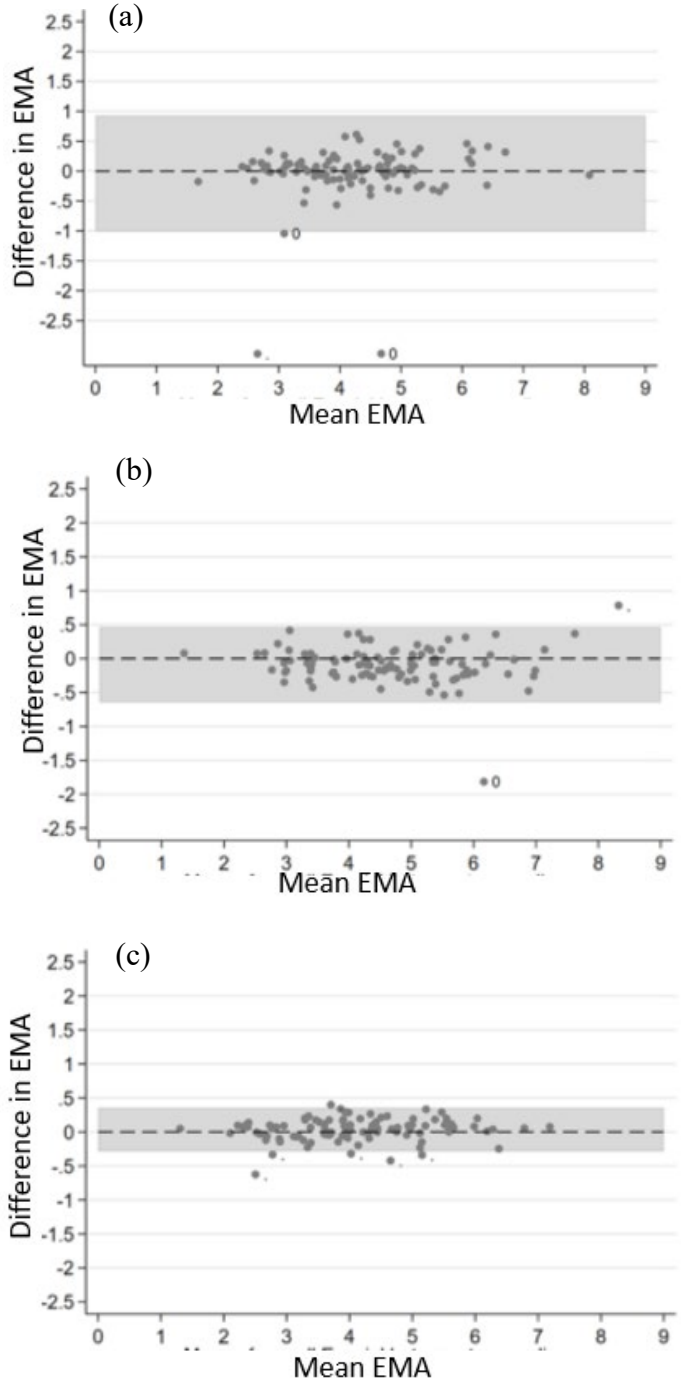

Figure 9: Bland-Altman Plots Showing the Intra-Rater Reliability for EMA Measured Within Observers At Least 1 Month Apart: (a) Rater EMG; (b) Rater JMQ; (c) Rater LHR.

Numerical values for bias and LoA are presented in Table 4. Overall, bias was minimal for each observer between time points (range –0.16 to 0.08). LoA were narrowest for the observer with the least radiology-specific training (LHR). Inter-rater reliability, bias and LoA for the averaged REMA, LEMA and EMA from both time points are summarized in Table 5 and Figure 10. CCCs between observers were poorer than within observers for all observer comparisons for REMA, LEMA and EMA (range 0.85– 0.94). Bias was increased when comparing measurements between observers vs. measurements by the same observer at different timepoints (range –0.46 to 0.66). The largest positive bias occurred between observers JQ and LR (0.58–0.66), and the largest negative bias occurred between observers EG and JQ (–0.44 to –0.46). The width of the LoA was similar for comparisons between all observers.

Table 5: Inter-Rater Reliability Assessed by Concordance Correlation Coefficient (CCC) and Bias (n = 101 CT Scans)*

Rater	REMA		LEMA		EMA	
	CCC (95% CI)	*Bias (95% LoA)*	*CCC (95% CI)*	*Bias (95% LoA)*	*CCC (95% CI)*	*Bias (95% LoA)*
EG vs. JQ	0.88 (0.85-0.92)	-0.44 (-1.19, 0.32)	0.87 (0.84-0.91)	-0.46 (-1.21, 0.30)	0.88 (0.85-0.92)	-0.45 (-1.16, 0.27)
EG vs. LR	0.94 (0.91-0.96)	0.15 (-0.59, 0.88)	0.93 (0.90-0.95)	0.20 (-0.55, 0.94)	0.94 (0.92-0.96)	0.17 (-0.51, 0.85)
JQ vs. LR	0.88 (0.84-0.91)	0.58 (0.14, 1.03)	0.85 (0.81-0.89)	0.66 (0.18, 1.13)	0.87 (0.83-0.90)	0.62 (0.20, 1.04)

The two readings from each rater were averaged due to high intra-rater reliability. N = 101 feline CT scans.

*The two readings from each rater were averaged due to high intra-rater reliability

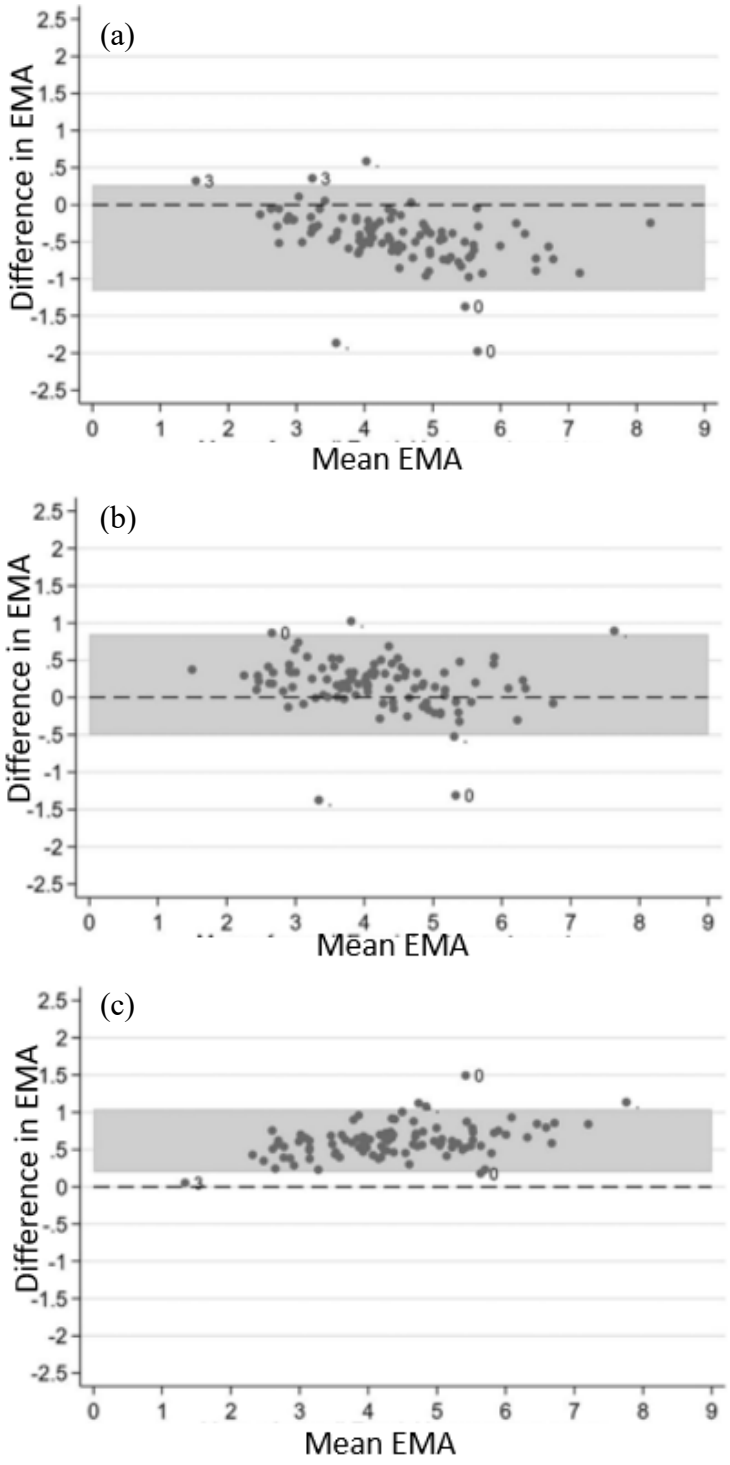

Figure 10: Bland–Altman Plots Showing the Inter-Rater Reliability for EMA: (a) Rater EMG vs JMQ; (b) Rater EMG vs LHR; (c) Rater JMQ vs LHR. Muscle Condition Score is Indicated for Outlying Points, When Available. n = 101 Feline CT Scans.

Box plots of the EMA for each muscle condition category are shown in Figure 11. Results of EMA for each observer and the average for all observers were compared for cats with different MCSs (Table 6). Descriptively speaking, median EMA was consistently lower in the severe atrophy group than other MCS groups for all three observers at both time points, but none of these comparisons reached statistical significance at P <0.05. When looking at the overall data across observers and time points, a significant difference in median EMA was observed between MCS groups. Post-hoc pairwise comparison revealed that the severe muscle atrophy group had significantly lower median values than the groups with no, mild and moderate muscle atrophy noted (all three P values <0.0001).

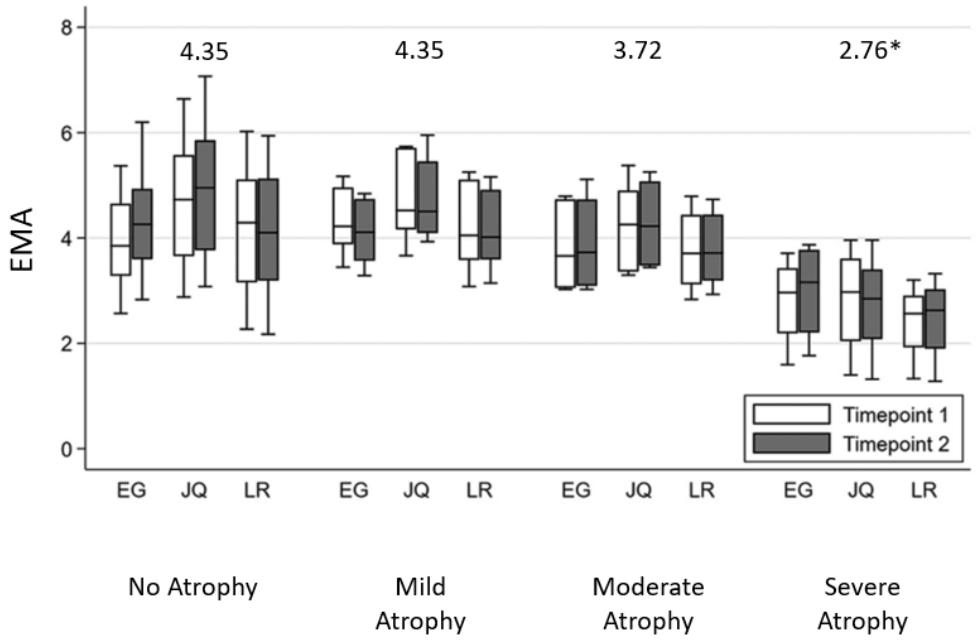

Figure 11: Box-and-Whisker Plots of EMA for Cats with Known Muscle Condition for Each Rater at Each Time Point. Numerical Values are Mean EMA for Each Muscle Condition Category. Values With an Asterisk are Significantly Different (P < 0.0001).

Table 6: Comparison of EMA According to Severity of Muscle Atrophy. Data are median (range).

Rater	Time Point	Muscle Atrophy				P-value
		None (n = 14)	*Mild (n = 6)*	*Moderate (n = 5)*	*Severe (n = 4)*	
EG	1	3.85 (2.57, 5.37)	4.22 (3.45, 5.17)	3.66 (3.02, 4.79)	2.96 (1.6, 3.71)	0.12
	2	4.26 (2.83, 6.20)	4.11 (3.28, 4.84)	3.73 (3.02, 5.11)	3.16 (1.77, 3.87)	0.30
JQ	1	4.73 (2.88, 6.64)	4.52 (3.66, 5.74)	4.25 (3.3, 5.38)	2.97 (1.4, 3.96)	0.058
	2	4.95 (3.08, 7.07)	4.50 (3.93, 5.95)	4.22 (3.44, 5.25)	2.85 (1.32, 3.96)	0.053
LR	1	4.29 (2.27, 6.02)	4.05 (3.08, 5.25)	3.71 (2.83, 4.79)	2.56 (1.33, 3.2)	0.066
	2	4.10 (2.17, 5.94)	4.02 (3.14, 5.16)	3.72 (2.93, 4.73)	2.62 (1.28, 3.32)	0.081
Overall		4.35[a] (2.17, 7.07)	4.35[a] (3.08, 5.95)	3.72[a] (2.83, 5.38)	2.76[b] (1.28, 3.96)	<0.001

[a, b] Within the same line, values with different superscripts are significantly different via Wilcoxon Ran Sum test at the P < 0.0001 level.

Information on final diagnosis was available for 100/101 cats, and a definitive diagnosis was reached in 96 cats. Forty-three cats had one comorbidity, 15 cats had two comorbidities and four cats had three comorbidities at the time of the CT scan. Sixty-two cats had a diagnosis of neoplastic disease at the time of the CT scan, and five cats had two or more forms of neoplasia. One cat had a meningioma with pulmonary nodules, which may have been metastatic or primary pulmonary neoplasia.

Discussion

The results of this study demonstrated that measurement of EMA on CT images showed moderate to substantial agreement when the same observer performed the measurement at different times. Agreement was poorer when compared between observers. The side of the epaxial musculature measured did not have a significant effect on intra- or inter-rater reliability of the measurement. Radiology-specific training did not appear to influence these results, and the highest intra-rater CCC values occurred between the observers with the most (EMG) and least (LHR) radiology-specific training. This indicates that this measurement technique could be performed with consistency, even by clinicians without specific training in radiographic techniques, and could be useful in quantifying muscle mass in cats undergoing CT scan.

More bias was identified between different observers compared with one observer repeating the measurement. The largest bias identified between observers in this study was 0.66 (JMQ vs LHR, LEMA). Cats assessed to have severe muscle wasting had a median EMA of just 2.76, and the smallest EMA measured in this study was 1.02. An inter-rater bias of 0.66 represents a large percentage of the EMA of cats with very little epaxial musculature. Thus, bias between two different observers is likely to be unacceptably large if the EMA is being used in a research setting or to track muscle mass changes within a single cat. Therefore, for optimal consistency, it would be recommended to have a single observer perform measurements to compare cats with each other or to track changes in muscle condition in a single cat over time. However, it is

unclear what effect training in the method would have on reliability between observers; perhaps with practice different observers would be able to achieve better agreement for the EMA than was found in the current study. Additionally, in the Bland–Altman plots comparing EMG with JMQ and JMQ with LHR, the magnitude of the bias appears to increase as the EMA increases (proportional bias). As such, calculating a single value for bias as the average difference between raters may over- or underestimate actual bias depending on the magnitude of the measured EMA.

Upon initial review of the CT images, a concern was that cats with more severe muscle wasting would be more difficult to measure and would produce greater differences between observers. Although the subset of cats with recorded moderate or severe muscle wasting was too small for statistical analysis of reliability, the results shown in Figure 12 do not imply poorer inter-rater reliability with more severe muscle atrophy. On the contrary, the cats with reportedly normal muscle condition have subjectively greater sample variability in EMA, differences between time points and differences between observers. This may be due to the larger sample size in this group compared with other MCS groups or may be due to a stock physical examination template that existed during a portion of the study period that described adequate muscle condition. If this template was not changed appropriately by the clinician on each case, cats with muscle wasting could have been erroneously recorded as being normal.

Owing to the retrospective nature of the study, only a small subset of cats had information on MCS available for analysis. However, the data demonstrated a greater

decrease in EMA for cats with severe muscle atrophy than for all other groups (Figure 12 and Table 6). This finding may illustrate a difficulty in subjectively evaluating subtle differences in muscle condition until loss becomes severe, leading to an overlap in epaxial muscle indices between all but the most severely affected group.

Establishing CT-derived EMA as a sensitive marker for lean body mass could be a first step toward identifying prognostic indicators for treatment response in specific disease states, as well as possible areas of intervention to counteract cachexia. This pilot study represents the first step toward this research goal and shows that measurement of feline EMA can be repeatably performed by the same observer. Based on our data, it is unclear whether the poor ability of EMA to distinguish between MCS groups 0–2 represents a lack of sensitivity of the EMA, a high variability in subjective MCS scoring or a combination of these effects. To answer this question, further studies evaluating this method prospectively within specific diseases states in cats with varying degrees of muscle atrophy and compared with a 'gold standard' lean body mass measurement (such as DEXA) are needed.

This study is limited by its retrospective nature. The variety of disease processes that prompted the CT scans and the small number of cats with recorded MCSs prevented the assessment of differences in EMA according to disease process and severity. Information on MCS and BCS was not available for all cats, and final diagnosis, comorbid conditions, signalment, and CT scanner and technique used to obtain the images were not controlled. It cannot be determined whether differences in image quality obtained with the different

CT scanners in the study affected the raters' ability to precisely measure the EMA. Missing MCS data points may have affected the relationship of muscle condition as observed on physical examination to EMA, but it is unlikely that they affected the observers' ability to perform the measurements, which was the primary interest of the present study. Diagnostic work-up to determine the final diagnosis and comorbidities was also not controlled. The MCS conferred to the cats was subjective and availability was clinician-dependent, as, unfortunately, the importance of MCS documentation has yet to be fully adopted as a crucial part of physical examination.

Chapter 7: Future Directions

Research and clinical intervention into cachexia associated with CKD and other chronic diseases can only improve quality of life and decrease mortality in our veterinary patients. However, in small animals, this area of research is in its infancy. This chapter will outline potential future areas of research that can further this field.

Establishment of a Gold Standard Measure of Lean Body Mass

As stated in previous sections, the establishment of a "gold standard" measure of lean body mass in veterinary patients is difficult at best. A true gold standard measure would have the power to reliably differentiate skeletal muscle from other tissue types, would be sensitive enough to detect subtle changes in the amount of total body skeletal muscle mass, and ideally, have the ability to determine what muscle groups are most affected when skeletal muscle mass changes. An ideal gold standard measure would also be inexpensive, non-invasive, quick, and easy to perform in the clinical setting. Imaging of a single muscle group or single cross-sectional abdominal CT image may best meet these goals; however, further research is needed to determine whether this is true. As outlined above, current skeletal muscle mass estimates from DEXA or BIA rely on assumptions of

constant hydration of skeletal muscle mass, which may not apply to veterinary patients with CKD, neoplasia, or other severe or chronic diseases. If imaging modalities are used to estimate total skeletal muscle mass or volume, we also do not know what muscle group or image location may be the best surrogate for total-body skeletal muscle quantification. In humans, studies have established a good correlation between total body skeletal muscle mass and total skeletal muscle cross-sectional area at the level of the third lumbar vertebra.[21, 28] Similar studies are lacking in veterinary patients.

Veterinary studies could be performed that use whole-body CT or MRI imaging to determine whole-body skeletal muscle amounts. CT or ultrasound to determine the area of single muscle groups, or muscle areas within single cross-sectional images of the chest or abdomen, could be performed. These could then be statistically compared to whole-body skeletal muscle amounts to determine a "sentinel" muscle group or location that could best correlate to whole-body skeletal muscle amounts. Estimates of whole-body skeletal muscle mass made with imaging modalities like CT or MRI could also be compared to FFM measurements from DEXA or BIA, if available. Such a study could be performed on cats and dogs in various states of muscle atrophy, and within various disease states, to establish how muscle mass changes with disease and establish a best practice for quantifying skeletal muscle in different patient populations.

Establishing the Mechanisms of Cachexia in Veterinary Patients

The first step toward establishing possible interventions which may help to prevent development of cachexia is to establish the cellular pathways that lead to cachexia development. Such pathways are currently being elucidated in humans and in rodent studies, but whether these are preserved in canine and feline patients is unproven.

If the above imaging study were to be performed on cadavers, representative samples of muscle from cats and dogs with different types of chronic disease (CKD, cardiac disease, neoplasia, etc.) could be obtained at the time of imaging. Histopathology on the samples could show potential differences in fibrosis and adipose tissue infiltration with disease. RT-PCR techniques could also be performed on the samples to determine whether the transcription factors implicated in rodent models (discussed in chapters 4 and 5) follow similar patterns of upregulation and downregulation in canine and feline skeletal muscle. These patterns could be correlated to total body skeletal muscle mass within the cadaver, as well as with our sentinel muscle group(s). We could also use techniques like the RAAS fingerprint to determine whether angiotensin II may play a similar role in dogs and cats with CKD and cachexia. Comparisons and correlations between pro-atrophic transcription patterns and RAAS with severity of atrophy could be determined for "healthy" aging cats vs. cats with CKD, hypertrophic cardiomyopathy, and other diseases. One interesting possible direction would be to establish that similar mechanisms are involved in canine/feline cachexia so that these can be used as a model for human

cachexia. If this were successful, translational studies for interventional drugs may be possible.

Interventional Studies

The eventual goal of research in this field is to establish interventional therapies that can prevent or slow the progression of cachexia. In this way, quality of life may be preserved even as disease continues to progress, and humane euthanasia may be delayed until more advanced stages of disease. Multiple therapeutic targets may exist, and one or a combination of these targets may allow for improvement in muscle condition and quality of life for our patients.

Multiple pharmacologic inhibitors of myostatin have been developed for use in human patients.[96] These include monoclonal antibodies specific to myostatin, as well as competitive inhibitors that bind the activin receptor (thereby inhibiting the activities of myostatin and activin simultaneously). Only one myostatin inhibitor has been evaluated in dogs (described above), and none have been evaluated in cats. As these drugs become more readily available, safety and efficacy studies could be performed for these myostatin inhibitors, using our previously established "sentinel" muscle group or location to determine whether their use allows for preservation or increase in skeletal muscle amounts.

PPAR-γ receptor agonists may have effects to decrease muscle atrophy via decreasing mitochondrial damage and generation of reactive oxygen species, as well as decreasing intracellular pro-inflammatory processes.[138] While the study establishing this in mouse models used a drug called rosiglitazone, a drug in the same class called pioglitazone has been evaluated in cats.[165] Pharmacokinetics of pioglitazone in lean and obese cats have been studied, and an efficacy study evaluating pioglitazone for its insulin-sensitizing and lipid-lowering effects in obese cats has also been performed.[166] Pioglitazone's effects on skeletal muscle were not evaluated in that study, but no adverse effects were identified at therapeutic dosages, so studies evaluating pioglitazone as an anti-cachectic drug could be safely performed in cats. Pharmacokinetic studies on pioglitazone have also been performed in Beagles, and the metabolism of pioglitazone in dogs appears to differ from its metabolism in humans.[167, 168] The clinical significance of this difference, as well as the overall safety of pioglitazone in dogs, are unknown.

RAAS inhibition is another interesting therapeutic target for cachexia in dogs and cats. The angiotensin-converting enzyme inhibitors (ACEis) enalapril and benazepril, and the angiotensin II receptor antagonist telmisartan are widely used in dogs and cats as anti-hypertensive and anti-proteinuric therapies. However, their potential effects on skeletal muscle have not been evaluated. These therapies are common enough that it may be possible to retrospectively evaluate muscle condition through time with chronic use of these therapies in patients with kidney disease. However, a retrospective evaluation would not include a quantitative measure of muscle mass, and would rely on the presence of a subjective muscle condition score within the existing medical record. A prospective

study evaluating the effect of ACEis and/or telmisartan on skeletal muscle amount, using the "sentinel" as a marker for whole-body skeletal muscle change, is warranted in future. However, a reliable way to quantify skeletal muscle in cats and dogs is necessary before such a study can be performed.

Lastly, an under-used but potentially powerful therapeutic target is exercise. Rehabilitation and physical therapy programs for dogs and cats recovering from orthopedic and neurologic disease are becoming more popular, and more widely available, than ever before. However, the use of these types of therapies to improve quality of life in chronic metabolic diseases has not been evaluated. An at-home exercise program for dogs and cats with CKD could potentially be implemented for owners to follow, and its efficacy could be compared to cats and dogs that did not participate in said exercise program, again using the "sentinel" as a marker.

In conclusion, cachexia and muscle mass loss are important, but under-diagnosed features of chronic disease in veterinary patients. Pathways by which chronic disease leads to loss of skeletal muscle mass are being studied in rodent models and human medicine, but have yet to be established in dogs and cats. The study of cachexia in dogs and cats is in its infancy, and a gold standard tool to assess a patient for early or mild loss of skeletal muscle mass does not currently exist. The first step in furthering his field of research in veterinary medicine is to establish fast, inexpensive, and non-invasive ways to assess or estimate total body skeletal muscle mass so that subtle changes can be identified and tracked. Our pilot study showed that evaluation of the epaxial muscle group cross

sectional area at the level of the TL junction, normalized to vertebral body height (EMA) is repeatable within observers, and is significantly lower in cats with severe muscle wasting on physical examination. Further studies are warranted to establish whether this is an ideal location and muscle group to act as a "sentinel" for total body skeletal muscle mass, and whether the EMA correlates well to other FFM measures. Once an appropriate "sentinel" is established, studies evaluating mechanisms associated with cachexia in dogs and cats, as well as potential therapeutic interventions, are warranted and may help to prevent debilitation in veterinary patients with chronic disease.

Bibliography

1. Freeman LM. Cachexia and Sarcopenia: Emerging Syndromes of Importance in Dogs and Cats. *J Vet Intern Med*. 2012; 26: 3-17.
2. Ahmadi SF, Zahmatkesh G, Ahmadi E, et al. Association of Body Mass Index with Clinical Outcomes in Non-Dialysis-Dependent Chronic Kidney Disease: A Systematic Review and Meta-Analysis. *Cardiorenal Med*. 2015; 6: 37-49.
3. Ahmadi SF, Zahmatkesh G, Streja E, et al. Association of Body Mass Index With Mortality in Peritoneal Dialysis Patients: A Systematic Review and Meta-Analysis. *Perit Dial Int*. 2016; 36: 315-25.
4. Harada K, Suzuki S, Ishii H, et al. Impact of Skeletal Muscle Mass on Long-Term Adverse Cardiovascular Outcomes in Patients With Chronic Kidney Disease. *Am J Cardiol*. 2017; 119: 1275-80.
5. Isoyama N, Qureshi AR, Avesani CM, et al. Comparative associations of muscle mass and muscle strength with mortality in dialysis patients. *Clin J Am Soc Nephrol*. 2014; 9: 1720-8.
6. Kim EY, Lee HY, Kim YS, et al. Prognostic significance of cachexia score assessed by CT in male patients with small cell lung cancer. *Eur J Cancer Care (Engl)*. 2018; 27.
7. Lu JL, Kalantar-Zadeh K, Ma JZ, Quarles LD and Kovesdy CP. Association of body mass index with outcomes in patients with CKD. *J Am Soc Nephrol*. 2014; 25: 2088-96.
8. Lu JL, Molnar MZ, Naseer A, Mikkelsen MK, Kalantar-Zadeh K and Kovesdy CP. Association of age and BMI with kidney function and mortality: a cohort study. *Lancet Diabetes Endocrinol*. 2015; 3: 704-14.
9. McDonald MN, Wouters EFM, Rutten E, et al. It's more than low BMI: prevalence of cachexia and associated mortality in COPD. *Respir Res*. 2019; 20: 100.
10. Prado CM, Baracos VE, McCargar LJ, et al. Sarcopenia as a determinant of chemotherapy toxicity and time to tumor progression in metastatic breast cancer patients receiving capecitabine treatment. *Clin Cancer Res*. 2009; 15: 2920-6.
11. Prado CM, Lieffers JR, McCargar LJ, et al. Prevalence and clinical implications of sarcopenic obesity in patients with solid tumours of the respiratory and gastrointestinal tracts: a population-based study. *Lancet Oncol*. 2008; 9: 629-35.
12. Tsekoura M, Kastrinis A, Katsoulaki M, Billis E and Gliatis J. Sarcopenia and Its Impact on Quality of Life. Cham: Springer International Publishing, 2017, p. 213-8.

13. Ineson DL, Freeman LM and Rush JE. Clinical and laboratory findings and survival time associated with cardiac cachexia in dogs with congestive heart failure. *J Vet Intern Med*. 2019; 33: 1902-8.
14. Baez JL, Michel KE, Sorenmo K and Shofer FS. A prospective investigation of the prevalence and prognostic significance of weight loss and changes in body condition in feline cancer patients. *J Feline Med Surg*. 2007; 9: 411-7.
15. Finn E, Freeman LM, Rush JE and Lee Y. The relationship between body weight, body condition, and survival in cats with heart failure. *J Vet Intern Med*. 2010; 24: 1369-74.
16. Freeman LM, Lachaud MP, Matthews S, Rhodes L and Zollers B. Evaluation of Weight Loss Over Time in Cats with Chronic Kidney Disease. *J Vet Intern Med*. 2016; 30: 1661-6.
17. Santiago SL, Freeman LM and Rush JE. Cardiac cachexia in cats with congestive heart failure: Prevalence and clinical, laboratory, and survival findings. *J Vet Intern Med*. 2020; 34: 35-44.
18. Michel KE, Anderson W, Cupp C and Laflamme DP. Correlation of a feline muscle mass score with body composition determined by dual-energy X-ray absorptiometry. *Br J Nutr*. 2011; 106 Suppl 1: S57-9.
19. Freeman LM, Becvarova I, Cave N, et al. WSAVA Nutrition Assessment Guidelines. *J Small Anim Pract*. 2011; 00.
20. Baracos VE, Reiman T, Mourtzakis M, Gioulbasanis I and Antoun S. Body composition in patients with non-small cell lung cancer: a contemporary view of cancer cachexia with the use of computed tomography image analysis. *Am J Clin Nutr*. 2010; 91: 1133S-7S.
21. Engelke K, Museyko O, Wang L and Laredo JD. Quantitative analysis of skeletal muscle by computed tomography imaging-State of the art. *J Orthop Translat*. 2018; 15: 91-103.
22. Goodpaster BH, Thaete FL and Kelley DE. Composition of Skeletal Muscle Evaluated with Computed Tomography. *Ann N Y Acad Sci*. 2006; 904.
23. Hernandez-Socorro CR, Saavedra P, Lopez-Fernandez JC and Ruiz-Santana S. Assessment of Muscle Wasting in Long-Stay ICU Patients Using a New Ultrasound Protocol. *Nutrients*. 2018; 10.
24. Heymsfield SB, Adamek M, Gonzalez MC, Jia G and Thomas DM. Assessing skeletal muscle mass: historical overview and state of the art. *J Cachexia Sarcopenia Muscle*. 2014; 5: 9-18.
25. Ismail C, Zabal J, Hernandez HJ, et al. Diagnostic ultrasound estimates of muscle mass and muscle quality discriminate between women with and without sarcopenia. *Front Physiol*. 2015; 6: 302.
26. Kim JS, Kim WY, Park HK, Kim MC, Jung W and Ko BS. Simple Age Specific Cutoff Value for Sarcopenia Evaluated by Computed Tomography. *Ann Nutr Metab*. 2017; 71: 157-63.
27. McClellan T, Allen BC, Kappus M, et al. Repeatability of Computerized Tomography-Based Anthropomorphic Measurements of Frailty in Patients With Pulmonary Fibrosis Undergoing Lung Transplantation. *Curr Probl Diagn Radiol*. 2017; 46: 300-4.

28. Mitsiopoulos N, Baumgartner RN, Heymsfield SB, Lyons W, Gallagher D and Ross R. Cadaver validation of skeletal muscle measurement by magnetic resonance imaging and computerized tomography. *J Appl Physiol (1985)*. 1998; 85: 115-22.
29. Morrell GR, Ikizler TA, Chen X, et al. Psoas Muscle Cross-sectional Area as a Measure of Whole-body Lean Muscle Mass in Maintenance Hemodialysis Patients. *J Ren Nutr*. 2016; 26: 258-64.
30. Mourtzakis M, Prado CM, Lieffers JR, Reiman T, McCargar LJ and Baracos VE. A practical and precise approach to quantification of body composition in cancer patients using computed tomography images acquired during routine care. *Appl Physiol Nutr Metab*. 2008; 33: 997-1006.
31. Nijholt W, Scafoglieri A, Jager-Wittenaar H, Hobbelen JSM and van der Schans CP. The reliability and validity of ultrasound to quantify muscles in older adults: a systematic review. *J Cachexia Sarcopenia Muscle*. 2017; 8: 702-12.
32. Perkisas S, Baudry S, Bauer J, et al. Application of ultrasound for muscle assessment in sarcopenia: towards standardized measurements. *European Geriatric Medicine*. 2018; 9: 739-57.
33. Schweitzer L, Geisler C, Pourhassan M, et al. What is the best reference site for a single MRI slice to assess whole-body skeletal muscle and adipose tissue volumes in healthy adults? *Am J Clin Nutr*. 2015; 102: 58-65.
34. Shen W, Punyanitya M, Wang Z, et al. Total body skeletal muscle and adipose tissue volumes: estimation from a single abdominal cross-sectional image. *J Appl Physiol*. 2004; 97: 2333-8.
35. Tillquist M, Kutsogiannis DJ, Wischmeyer PE, et al. Bedside ultrasound is a practical and reliable measurement tool for assessing quadriceps muscle layer thickness. *JPEN J Parenter Enteral Nutr*. 2014; 38: 886-90.
36. van Vugt JL, Levolger S, Gharbharan A, et al. A comparative study of software programmes for cross-sectional skeletal muscle and adipose tissue measurements on abdominal computed tomography scans of rectal cancer patients. *J Cachexia Sarcopenia Muscle*. 2017; 8: 285-97.
37. Cederholm T, Barazzoni R, Austin P, et al. ESPEN guidelines on definitions and terminology of clinical nutrition. *Clin Nutr*. 2017; 36: 49-64.
38. Cederholm T, Bosaeus I, Barazzoni R, et al. Diagnostic criteria for malnutrition - An ESPEN Consensus Statement. *Clin Nutr*. 2015; 34: 335-40.
39. Barendregt K, Soeters P, Allison S and Sobotka L. Basics in clinical nutrition: Simple and stress starvation. *E Spen Eur E J Clin Nutr Metab*. 2008; 3: e267-e71.
40. Dev R. Measuring cachexia-diagnostic criteria. *Ann Palliat Med*. 2019; 8: 24-32.
41. Argiles JM, Betancourt A, Guardia-Olmos J, et al. Validation of the CAchexia SCOre (CASCO). Staging Cancer Patients: The Use of miniCASCO as a Simplified Tool. *Front Physiol*. 2017; 8: 92.
42. Blum D, Stene GB, Solheim TS, et al. Validation of the Consensus-Definition for Cancer Cachexia and evaluation of a classification model--a study based on data from an international multicentre project (EPCRC-CSA). *Ann Oncol*. 2014; 25: 1635-42.
43. Dawson-Hughes B and Bischoff-Ferrari H. Considerations concerning the definition of sarcopenia. *Osteoporos Int*. 2016; 27: 3139-44.

44. Sanchez-Rodriguez D, Marco E and Cruz-Jentoft AJ. Defining sarcopenia: some caveats and challenges. *Curr Opin Clin Nutr Metab Care*. 2019.
45. Cruz-Jentoft AJ, Baeyens JP, Bauer JM, et al. Sarcopenia: European consensus on definition and diagnosis: Report of the European Working Group on Sarcopenia in Older People. *Age Ageing*. 2010; 39: 412-23.
46. Cruz-Jentoft AJ, Bahat G, Bauer J, et al. Sarcopenia: revised European consensus on definition and diagnosis. *Age Ageing*. 2019; 48: 16-31.
47. Muscaritoli M, Anker SD, Argiles J, et al. Consensus definition of sarcopenia, cachexia and pre-cachexia: joint document elaborated by Special Interest Groups (SIG) "cachexia-anorexia in chronic wasting diseases" and "nutrition in geriatrics". *Clin Nutr*. 2010; 29: 154-9.
48. Robinson S, Granic A and Sayer AA. Nutrition and Muscle Strength, As the Key Component of Sarcopenia: An Overview of Current Evidence. *Nutrients*. 2019; 11.
49. Evans WJ, Morley JE, Argiles J, et al. Cachexia: a new definition. *Clin Nutr*. 2008; 27: 793-9.
50. Locquet M, Beaudart C, Reginster JY, Petermans J and Bruyere O. Comparison of the performance of five screening methods for sarcopenia. *Clin Epidemiol*. 2018; 10: 71-82.
51. Locquet M, Beaudart C, Hajaoui M, Petermans J, Reginster JY and Bruyere O. Three-Year Adverse Health Consequences of Sarcopenia in Community-Dwelling Older Adults According to 5 Diagnosis Definitions. *J Am Med Dir Assoc*. 2019; 20: 43-6 e2.
52. Freeman LM, Michel KE, Zanghi BM, Vester Boler BM and Fages J. Evaluation of the use of muscle condition score and ultrasonographic measurements for assessment of muscle mass in dogs. *Am J Vet Res*. 2019; 80: 595-600.
53. Stenholm S, Harris TB, Rantanen T, Visser M, Kritchevsky SB and Ferrucci L. Sarcopenic obesity: definition, cause and consequences. *Curr Opin Clin Nutr Metab Care*. 2008; 11: 693-700.
54. Lee DC, Shook RP, Drenowatz C and Blair SN. Physical activity and sarcopenic obesity: definition, assessment, prevalence and mechanism. *Future Sci OA*. 2016; 2: FSO127.
55. Fouque D, Kalantar-Zadeh K, Kopple J, et al. A proposed nomenclature and diagnostic criteria for protein-energy wasting in acute and chronic kidney disease. *Kidney Int*. 2008; 73: 391-8.
56. Carrero JJ, Stenvinkel P, Cuppari L, et al. Etiology of the protein-energy wasting syndrome in chronic kidney disease: a consensus statement from the International Society of Renal Nutrition and Metabolism (ISRNM). *J Ren Nutr*. 2013; 23: 77-90.
57. Reid J, Noble HR, Slee A, et al. Distinguishing Between Cachexia, Sarcopenia and Protein Energy Wasting in End-Stage Renal Disease Patients on Dialysis. *Palliative Medicine and Hospice Care - Open Journal*. 2016; 2: e11-e3.
58. Gracia-Iguacel C, Gonzalez-Parra E, Barril-Cuadrado G, et al. Defining protein-energy wasting syndrome in chronic kidney disease: prevalence and clinical implications. *Nefrología*. 2014; 34: 507-19.
59. Carrero JJ, Thomas F, Nagy K, et al. Global Prevalence of Protein-Energy Wasting in Kidney Disease: A Meta-analysis of Contemporary Observational Studies

From the International Society of Renal Nutrition and Metabolism. *J Ren Nutr*. 2018; 28: 380-92.
60. Komaba H and Fukagawa M. Secondary Hyperparathyroidism and Protein-Energy Wasting in End-Stage Renal Disease. *Ther Apher Dial*. 2018; 22: 246-50.
61. Lim SL, Lin XH and Daniels L. Seven-Point Subjective Global Assessment Is More Time Sensitive Than Conventional Subjective Global Assessment in Detecting Nutrition Changes. *JPEN J Parenter Enteral Nutr*. 2016; 40: 966-72.
62. Kalantar-Zadeh K, Kopple JD, Block G and Humphreys MH. A malnutrition-inflammation score is correlated with morbidity and mortality in maintenance hemodialysis patients. *Am J Kidney Dis*. 2001; 38: 1251-63.
63. Fearon K, Strasser F, Anker SD, et al. Definition and classification of cancer cachexia: an international consensus. *Lancet Oncol*. 2011; 12: 489-95.
64. Argiles JM, Lopez-Soriano FJ, Toledo M, Betancourt A, Serpe R and Busquets S. The cachexia score (CASCO): a new tool for staging cachectic cancer patients. *J Cachexia Sarcopenia Muscle*. 2011; 2: 87-93.
65. Anker SD and Coats AJ. Cardiac cachexia: a syndrome with impaired survival and immune and neuroendocrine activation. *Chest*. 1999; 115: 836-47.
66. Frontera WR and Ochala J. Skeletal muscle: a brief review of structure and function. *Calcif Tissue Int*. 2015; 96: 183-95.
67. Schiaffino S, Dyar KA, Ciciliot S, Blaauw B and Sandri M. Mechanisms regulating skeletal muscle growth and atrophy. *FEBS J*. 2013; 280: 4294-314.
68. Hermanson JW and Evans HE. The Muscular System. *Miller's Anatomy of the Dog*. 3 ed. Philadelphia, PA: Saunders, 1993, p. 259-384.
69. Biga LM, Dawson S, Harwell A, et al. Skeletal Muscle. *Anatomy & Physiology*. OpenStax/Oregon State University, p. 909-23.
70. Costanzo LS. Skeletal Muscle. *Physiology*. 6 ed. Philadelphia, PA: Elsevier, 2018, p. xi, 516 pages.
71. Hall JE. Contraction of Skeletal Muscle. *Guyton and Hall Textbook of Medical Physiology*. 13 ed. Philadelphia, PA: Elsevier, 2016, p. 75-88.
72. Scott W, Stevens J and Binder-Macleod SA. Human skeletal muscle fiber type classifications. *Phys Ther*. 2001; 81: 1810-6.
73. Goodman CA. The role of mTORC1 in regulating protein synthesis and skeletal muscle mass in response to various mechanical stimuli. *Rev Physiol Biochem Pharmacol*. 2014; 166: 43-95.
74. Bilodeau PA, Coyne ES and Wing SS. The ubiquitin proteasome system in atrophying skeletal muscle: roles and regulation. *Am J Physiol Cell Physiol*. 2016; 311: C392-403.
75. Laplante M and Sabatini DM. mTOR signaling in growth control and disease. *Cell*. 2012; 149: 274-93.
76. Bentzinger CF, Lin S, Romanino K, et al. Differential response of skeletal muscles to mTORC1 signaling during atrophy and hypertrophy. *Skelet Muscle*. 2013; 3: 6.
77. Ogasawara R, Jensen TE, Goodman CA and Hornberger TA. Resistance Exercise-Induced Hypertrophy: A Potential Role for Rapamycin-Insensitive mTOR. *Exerc Sport Sci Rev*. 2019; 47: 188-94.

78. Cunningham JT, Rodgers JT, Arlow DH, Vazquez F, Mootha VK and Puigserver P. mTOR controls mitochondrial oxidative function through a YY1-PGC-1alpha transcriptional complex. *Nature*. 2007; 450: 736-40.
79. Su KH and Dai C. mTORC1 senses stresses: Coupling stress to proteostasis. *Bioessays*. 2017; 39.
80. Kenney DL and Benarroch EE. The autophagy-lysosomal pathway: General concepts and clinical implications. *Neurology*. 2015; 85: 634-45.
81. Bodine SC, Stitt TN, Gonzalez MC, et al. Akt/mTOR pathway is a crucial regulator of skeletal muscle hypertrophy and can prevent muscle atrophy in vivo. *Nature Cell Biology*. 2001; 3: 1014-9.
82. Hall JE. Pituitary Hormones and Their Control by the Hypothalamus. *Guyton and Hall Textbook of Medical Physiology*. 13 ed. Philadelphia, PA: Elsevier, 2016, p. 939-50.
83. Feldman EC, Nelson RW, Reusch C and Scott-Moncrieff JCR. Disorders of Growth Hormone. *Canine & Feline Endocrinology*. 4 ed. St. Louis, Missouri: Elsevier Saunders, 2015, p. 37-76.
84. Dardevet D, Manin M, Balage M, Sornet C and Grizard J. Influence of low- and high-protein diets on insulin and insulin-like growth factor-1 binding to skeletal muscle and liver in the growing rat. *Br J Nutr*. 1991; 65: 47-60.
85. Clemmons DR. Metabolic actions of insulin-like growth factor-I in normal physiology and diabetes. *Endocrinol Metab Clin North Am*. 2012; 41: 425-43, vii-viii.
86. Favier FB, Costes F, Defour A, et al. Downregulation of Akt/mammalian target of rapamycin pathway in skeletal muscle is associated with increased REDD1 expression in response to chronic hypoxia. *Am J Physiol Regul Integr Comp Physiol*. 2010; 298: R1659-66.
87. Thrower JS, Hoffman L, Rechsteiner M and Pickart CM. Recognition of the polyubiquitin proteolytic signal. *EMBO J*. 2000; 19: 94-102.
88. Iconomou M and Saunders DN. Systematic approaches to identify E3 ligase substrates. *Biochem J*. 2016; 473: 4083-101.
89. Mizushima N, Yoshimori T and Ohsumi Y. The role of Atg proteins in autophagosome formation. *Annu Rev Cell Dev Biol*. 2011; 27: 107-32.
90. Kruppa AJ, Kendrick-Jones J and Buss F. Myosins, Actin and Autophagy. *Traffic*. 2016; 17: 878-90.
91. Verzola D, Procopio V, Sofia A, et al. Apoptosis and myostatin mRNA are upregulated in the skeletal muscle of patients with chronic kidney disease. *Kidney Int*. 2011; 79: 773-82.
92. Cabello-Verrugio C, Cordova G and Salas JD. Angiotensin II: role in skeletal muscle atrophy. *Curr Protein Pept Sci*. 2012; 13: 560-9.
93. Zheng B, Ohkawa S, Li H, Roberts-Wilson TK and Price SR. FOXO3a mediates signaling crosstalk that coordinates ubiquitin and atrogin-1/MAFbx expression during glucocorticoid-induced skeletal muscle atrophy. *FASEB J*. 2010; 24: 2660-9.
94. Song Y-H, Li Y, Du J, Mitch WE, Rosenthal N and Delafontaine P. Muscle-specific expression of IGF-1 blocks angiotensin II–induced skeletal muscle wasting. *Journal of Clinical Investigation*. 2005; 115: 451-8.

95. Verzola D, Bonanni A, Sofia A, et al. Toll-like receptor 4 signalling mediates inflammation in skeletal muscle of patients with chronic kidney disease. *J Cachexia Sarcopenia Muscle*. 2017; 8: 131-44.
96. Verzola D, Barisione C, Picciotto D, Garibotto G and Koppe L. Emerging role of myostatin and its inhibition in the setting of chronic kidney disease. *Kidney Int*. 2019; 95: 506-17.
97. Boman IA, Klemetsdal G, Blichfeldt T, Nafstad O and Vage DI. A frameshift mutation in the coding region of the myostatin gene (MSTN) affects carcass conformation and fatness in Norwegian White Sheep (Ovis aries). *Anim Genet*. 2009; 40: 418-22.
98. McPherron AC and Lee SJ. Double muscling in cattle due to mutations in the myostatin gene. *Proc Natl Acad Sci U S A*. 1997; 94: 12457-61.
99. Mosher DS, Quignon P, Bustamante CD, et al. A mutation in the myostatin gene increases muscle mass and enhances racing performance in heterozygote dogs. *PLoS Genet*. 2007; 3: e79.
100. Schuelke M, Wagner KR, Stolz LE, et al. Myostatin mutation associated with gross muscle hypertrophy in a child. *N Engl J Med*. 2004; 350: 2682-8.
101. Chen JL, Walton KL, Winbanks CE, et al. Elevated expression of activins promotes muscle wasting and cachexia. *FASEB J*. 2014; 28: 1711-23.
102. Goodman CA, McNally RM, Hoffmann FM and Hornberger TA. Smad3 induces atrogin-1, inhibits mTOR and protein synthesis, and promotes muscle atrophy in vivo. *Mol Endocrinol*. 2013; 27: 1946-57.
103. Ding H, Zhang G, Sin KW, et al. Activin A induces skeletal muscle catabolism via p38beta mitogen-activated protein kinase. *J Cachexia Sarcopenia Muscle*. 2017; 8: 202-12.
104. Dong J, Dong Y, Chen Z, Mitch WE and Zhang L. The pathway to muscle fibrosis depends on myostatin stimulating the differentiation of fibro/adipogenic progenitor cells in chronic kidney disease. *Kidney Int*. 2017; 91: 119-28.
105. Yano S, Nagai A, Isomura M, et al. Relationship between Blood Myostatin Levels and Kidney Function:Shimane CoHRE Study. *PLoS One*. 2015; 10: e0141035.
106. Zhang L, Pan J, Dong Y, et al. Stat3 activation links a C/EBPdelta to myostatin pathway to stimulate loss of muscle mass. *Cell Metab*. 2013; 18: 368-79.
107. Zhang L, Rajan V, Lin E, et al. Pharmacological inhibition of myostatin suppresses systemic inflammation and muscle atrophy in mice with chronic kidney disease. *FASEB J*. 2011; 25: 1653-63.
108. Anders HJ, Andersen K and Stecher B. The intestinal microbiota, a leaky gut, and abnormal immunity in kidney disease. *Kidney Int*. 2013; 83: 1010-6.
109. Jones KL, Mansell A, Patella S, et al. Activin A is a critical component of the inflammatory response, and its binding protein, follistatin, reduces mortality in endotoxemia. *Proc Natl Acad Sci U S A*. 2007; 104: 16239-44.
110. Bish LT, Sleeper MM, Forbes SC, et al. Long-term systemic myostatin inhibition via liver-targeted gene transfer in golden retriever muscular dystrophy. *Hum Gene Ther*. 2011; 22: 1499-509.
111. Cotten SW, Kornegay JN, Bogan DJ, Wadosky KM, Patterson C and Willis MS. Genetic myostatin decrease in the golden retriever muscular dystrophy model does not

significantly affect the ubiquitin proteasome system despite enhancing the severity of disease. *Am J Transl Res*. 2013; 6: 43-53.
112. Kornegay JN, Bogan DJ, Bogan JR, et al. Dystrophin-deficient dogs with reduced myostatin have unequal muscle growth and greater joint contractures. *Skelet Muscle*. 2016; 6: 14.
113. Freeman LM, Rush JE, Cunningham SM, Yang VK and Bulmer BJ. Pilot study of a myostatin antagonist in dogs with cardiac cachexia. *J Vet Cardiol*. 2015; 17: 210-5.
114. Bakkar N and Guttridge DC. NF-kappaB signaling: a tale of two pathways in skeletal myogenesis. *Physiol Rev*. 2010; 90: 495-511.
115. Cai D, Frantz JD, Tawa NE, Jr., et al. IKKbeta/NF-kappaB activation causes severe muscle wasting in mice. *Cell*. 2004; 119: 285-98.
116. Van Gammeren D, Damrauer JS, Jackman RW and Kandarian SC. The IkappaB kinases IKKalpha and IKKbeta are necessary and sufficient for skeletal muscle atrophy. *FASEB J*. 2009; 23: 362-70.
117. Mourkioti F, Kratsios P, Luedde T, et al. Targeted ablation of IKK2 improves skeletal muscle strength, maintains mass, and promotes regeneration. *J Clin Invest*. 2006; 116: 2945-54.
118. Hunter RB and Kandarian SC. Disruption of either the Nfkb1 or the Bcl3 gene inhibits skeletal muscle atrophy. *J Clin Invest*. 2004; 114: 1504-11.
119. Oh J, Sinha I, Tan KY, et al. Age-associated NF-kappaB signaling in myofibers alters the satellite cell niche and re-strains muscle stem cell function. *Aging (Albany NY)*. 2016; 8: 2871-96.
120. Zhang N, Valentine JM, Zhou Y, et al. Sustained NFkappaB inhibition improves insulin sensitivity but is detrimental to muscle health. *Aging Cell*. 2017; 16: 847-58.
121. Guijarro C and Egido J. Transcription factor-kappa B (NF-kappa B) and renal disease. *Kidney Int*. 2001; 59: 415-24.
122. Andrade-Oliveira V, Foresto-Neto O, Watanabe IKM, Zatz R and Camara NOS. Inflammation in Renal Diseases: New and Old Players. *Front Pharmacol*. 2019; 10: 1192.
123. Bhatnagar S and Kumar A. The TWEAK-Fn14 System: Breaking the Silence of Cytokine-Induced Skeletal Muscle Wasting. *Current Molecular Medicine*. 2012; 12: 3-13.
124. Bernardi S, Voltan R, Rimondi E, et al. TRAIL, OPG, and TWEAK in kidney disease: biomarkers or therapeutic targets? *Clin Sci (Lond)*. 2019; 133: 1145-66.
125. Javard R, Grimes C, Bau-Gaudreault L and Dunn M. Acute-Phase Proteins and Iron Status in Cats with Chronic Kidney Disease. *J Vet Intern Med*. 2017; 31: 457-64.
126. Nentwig A, Schweighauser A, Maissen-Villiger C, et al. Assessment of the expression of biomarkers of uremic inflammation in dogs with renal disease. *Am J Vet Res*. 2016; 77: 218-24.
127. Costanzo LS. Adrenal Medulla and Cortex. *Physiology*. 6 ed. Philadelphia, PA: Elsevier, 2018, p. xi, 516 pages.
128. Bodine SC and Furlow JD. Glucocorticoids and Skeletal Muscle. *Adv Exp Med Biol*. 2015; 872: 145-76.

129. May RC, Bailey JL, Mitch WE, Masud T and England BK. Glucocorticoids and acidosis stimulate protein and amino acid catabolism in vivo. *Kidney Int*. 1996; 49: 679-83.
130. Rosman PM, Farag A, Peckham R, et al. Pituitary-adrenocortical function in chronic renal failure: blunted suppression and early escape of plasma cortisol levels after intravenous dexamethasone. *J Clin Endocrinol Metab*. 1982; 54: 528-33.
131. Li X, Xiang X, Hu J, et al. Association Between Serum Cortisol and Chronic Kidney Disease in Patients with Essential Hypertension. *Kidney Blood Press Res*. 2016; 41: 384-91.
132. Costanzo LS. Regulation of Arterial Pressure. *Physiology*. 6 ed. Philadelphia, PA: Elsevier, 2018, p. xi, 516 pages.
133. Zhang L, Du J, Hu Z, et al. IL-6 and serum amyloid A synergy mediates angiotensin II-induced muscle wasting. *J Am Soc Nephrol*. 2009; 20: 604-12.
134. Brink M, Price SR, Chrast J, et al. Angiotensin II induces skeletal muscle wasting through enhanced protein degradation and down-regulates autocrine insulin-like growth factor I. *Endocrinology*. 2001; 142: 1489-96.
135. Yoshida T, Semprun-Prieto L, Sukhanov S and Delafontaine P. IGF-1 prevents ANG II-induced skeletal muscle atrophy via Akt- and Foxo-dependent inhibition of the ubiquitin ligase atrogin-1 expression. *Am J Physiol Heart Circ Physiol*. 2010; 298: H1565-70.
136. Silva KAS, Ghiarone T, Schreiber K, et al. Angiotensin II suppresses autophagy and disrupts ultrastructural morphology and function of mitochondria in mouse skeletal muscle. *J Appl Physiol (1985)*. 2019; 126: 1550-62.
137. Folli F, Kahn CR, Hansen H, Bouchie JL and Feener EP. Angiotensin II inhibits insulin signaling in aortic smooth muscle cells at multiple levels. A potential role for serine phosphorylation in insulin/angiotensin II crosstalk. *J Clin Invest*. 1997; 100: 2158-69.
138. Liu Y, Bi X, Zhang Y, Wang Y and Ding W. Mitochondrial dysfunction/NLRP3 inflammasome axis contributes to angiotensin II-induced skeletal muscle wasting via PPAR-gamma. *Lab Invest*. 2019.
139. Yoshida T, Tabony AM, Galvez S, et al. Molecular mechanisms and signaling pathways of angiotensin II-induced muscle wasting: potential therapeutic targets for cardiac cachexia. *Int J Biochem Cell Biol*. 2013; 45: 2322-32.
140. Du Bois P, Pablo Tortola C, Lodka D, et al. Angiotensin II Induces Skeletal Muscle Atrophy by Activating TFEB-Mediated MuRF1 Expression. *Circ Res*. 2015; 117: 424-36.
141. Swanson KV, Deng M and Ting JP. The NLRP3 inflammasome: molecular activation and regulation to therapeutics. *Nat Rev Immunol*. 2019; 19: 477-89.
142. Semprun-Prieto LC, Sukhanov S, Yoshida T, et al. Angiotensin II induced catabolic effect and muscle atrophy are redox dependent. *Biochem Biophys Res Commun*. 2011; 409: 217-21.
143. Lin YL, Chen SY, Lai YH, et al. Angiotensin II receptor blockade is associated with preserved muscle strength in chronic hemodialysis patients. *BMC Nephrol*. 2019; 20: 54.

144. Mishina M, Watanabe T, Fujii K, Maeda H, Wakao Y and Takahashi M. Non-invasive blood pressure measurements in cats: clinical significance of hypertension associated with chronic renal failure. *J Vet Med Sci*. 1998; 60: 805-8.
145. Mishina M and Watanabe T. Development of hypertension and effects of benazepril hydrochloride in a canine remnant kidney model of chronic renal failure. *J Vet Med Sci*. 2008; 70: 455-60.
146. Dumler F. Use of Bioelectric Impedance Analysis and Dual-Energy X-Ray Absorptiometry for Monitoring the Nutrition Status of Dialysis Patients. *ASAIO Journal*. 1997; 43: 256-60.
147. Tosato M, Marzetti E, Cesari M, et al. Measurement of muscle mass in sarcopenia: from imaging to biochemical markers. *Aging Clin Exp Res*. 2017; 29: 19-27.
148. Jeusette I, Greco D, Aquino F, et al. Effect of breed on body composition and comparison between various methods to estimate body composition in dogs. *Res Vet Sci*. 2010; 88: 227-32.
149. Lauten SD, Cox NR, Brawner WR, Jr. and Baker HJ. Use of dual energy x-ray absorptiometry for noninvasive body composition measurements in clinically normal dogs. *Am J Vet Res*. 2001; 62: 1295-301.
150. Raffan E, Holden SL, Cullingham F, Hackett RM, Rawlings JM and German AJ. Standardized positioning is essential for precise determination of body composition using dual-energy x-ray absorptiometry in dogs. *J Nutr*. 2006; 136: 1976S-8S.
151. Munday HS, Booles D, Anderson P, Poore DW and Earle KE. The repeatability of body composition measurements in dogs and cats using dual energy X-ray absorptiometry. *J Nutr*. 1994; 124: 2619S-21S.
152. Speakman JR, Booles D and Butterwick R. Validation of dual energy X-ray absorptiometry (DXA) by comparison with chemical analysis of dogs. *Int J Obes*. 2001; 25: 439-47.
153. Zanghi BM, Cupp CJ, Pan Y, et al. Noninvasive measurements of body composition and body water via quantitative magnetic resonance, deuterium water, and dual-energy x-ray absorptiometry in awake and sedated dogs. *Am J Vet Res*. 2013; 74: 733-43.
154. Rae LS, Vankan DM, Rand JS, Flickinger EA and Ward LC. Measuring body composition in dogs using multifrequency bioelectrical impedance analysis and dual energy X-ray absorptiometry. *Vet J*. 2016; 212: 65-70.
155. Stanton CA, Hamar DW, Johnson DE and Fettman MJ. Bioelectrical impedance and zoometry for body composition analysis in domestic cats. *Am J Vet Res*. 1992; 53: 251-7.
156. Gould DW, Watson EL, Wilkinson TJ, et al. Ultrasound assessment of muscle mass in response to exercise training in chronic kidney disease: a comparison with MRI. *J Cachexia Sarcopenia Muscle*. 2019; 10: 748-55.
157. Heymsfield SB, Gonzalez MC, Lu J, Jia G and Zheng J. Skeletal muscle mass and quality: evolution of modern measurement concepts in the context of sarcopenia. *Proc Nutr Soc*. 2015; 74: 355-66.
158. Hutchinson D, Sutherland-Smith J, Watson AL and Freeman LM. Assessment of methods of evaluating sarcopenia in old dogs. *Am J Vet Res*. 2012; 73: 1794-800.

159. Freeman LM, Sutherland-Smith J, Prantil LR, Sato AF, Rush JE and Barton BA. Quantitative assessment of muscle in dogs using a vertebral epaxial muscle score. *Can J Vet Res*. 2017; 81: 255-60.
160. Freeman LM, Sutherland-Smith J, Cummings C and Rush JE. Evaluation of a quantitatively derived value for assessment of muscle mass in clinically normal cats. *Am J Vet Res*. 2018; 79: 1188-92.
161. Mitchell AD. Validation of quantitative magnetic resonance body composition analysis for infants using piglet model. *Pediatr Res*. 2011; 69: 330-5.
162. Zanghi BM, Cupp CJ, Pan Y, et al. Noninvasive measurements of body composition and body water via quantitative magnetic resonance, deuterium water, and dual-energy x-ray absorptiometry in cats. *Am J Vet Res*. 2013; 74: 721-32.
163. Turner RBS, Hepworth G, Wilson K, Tyrrell D, Dunshea FR and Mansfield CS. Abdominal volume computed tomography assessment of body composition in dogs. *BMC Vet Res*. 2019; 15: 21.
164. Sutherland-Smith J, Hutchinson D and Freeman LM. Comparison of computed tomographic attenuation values for epaxial muscles in old and young dogs. *Am J Vet Res*. 2019; 80: 174-7.
165. Clark MH, Hoenig M, Ferguson DC and Dirikolu L. Pharmacokinetics of pioglitazone in lean and obese cats. *J Vet Pharmacol Ther*. 2012; 35: 428-36.
166. Clark M, Thomaseth K, Dirikolu L, Ferguson DC and Hoenig M. Effects of Pioglitazone on Insulin Sensitivity and Serum Lipids in Obese Cats. *J Vet Intern Med*. 2014; 28: 166-74.
167. Shen Z, Reed JR, Creighton M, et al. Identification of novel metabolites of pioglitazone in rat and dog. *Xenobiotica*. 2003; 33: 499-509.
168. Zhang X, Peng Y, Wan P, Yin L, Wang G and Sun J. Simultaneous determination and pharmacokinetic study of metformin and pioglitazone in dog plasma by LC-MS-MS. *J Chromatogr Sci*. 2014; 52: 52-8.